Available online at www.sciencedirect.com
ScienceDirect
Geochimica et Cosmochimica Acta 72 (2008) 3661–3680
Geochimica et Cosmochimica Acta
www.elsevier.com/locate/gca

Rapid releases of metal salts and nutrients following the deposition of volcanic ash into aqueous environments

Morgan T. Jones [a,*], Sigurður R. Gislason [b]

[a] Department of Earth Sciences, University of Bristol, Wills Memorial Building, Queens Road, Bristol BS8 1RJ, United Kingdom
[b] Institute of Earth Sciences, University of Iceland, Sturlugata 7, Reykjavik IS-101, Iceland

Received 30 August 2007; accepted in revised form 7 May 2008; available online 21 May 2008

Abstract

Deposition of volcanic ash into aqueous environments leads to dissolution of adsorbed metal salts and aerosols, increasing the bioavailability of key nutrients. Volcanogenic fertilization events could increase marine primary productivity, leading to a drawdown of atmospheric CO_2. Here we conduct flow-through experiments on unhydrated volcanic ash samples from a variety of locations and sources, measuring the concentrations and fluxes of elements into de-ionized water and two contrasting ocean surface waters. Comparisons of element fluxes show that dissolution of adsorbed surface salts and aerosols dominates over glass dissolution, even in sustained low pH conditions. These surface ash-leachates appear unstable, decaying in situ even if kept unhydrated. Volcanic ash from recent eruptions is shown to have a large fertilization potential in both fresh and saline water. Fluorine concentrations are integral to bulk dissolution rates and samples with high F concentrations display elevated fluxes of some nutrients, particularly Fe, Si, and P. Bio-limiting micronutrients are released in large quantities, suggesting that subsequent biological growth will be limited by macronutrient availability. Importantly, acidification of surface waters and high fluxes of toxic elements highlights the potential of volcanic ash-leachates to poison aqueous environments. In particular, large pH changes can cause undersaturation of $CaCO_3$ polymorphs, damaging populations of calcifying organisms. Deposition of volcanic ash can both fertilize and/or poison aqueous environments, causing significant changes to surface water chemistry and biogeochemical cycles.

1. INTRODUCTION

Explosive volcanic eruptions are capable of causing significant disruptions to the Earth's climate (Kelly et al., 1996; Robock, 2000). The environmental repercussions following volcanic eruptions are complex as many cycles in the Earth system are affected simultaneously. An important consideration is the release of gases, aerosols, and metal salts during an eruption, which have the ability to instigate rapid biogeochemical changes upon deposition. Acids, metal salts and adsorbed gases on tephra (airborne volcanic particulate matter) surfaces are highly soluble, dissolving rapidly on contact with water (Frogner et al., 2001). These soluble surface accumulations have been termed 'ash-leachates' by previous investigations (Witham et al., 2005) and we use this term herein. Ash-leachate chemistry and volume can vary considerably. Gas solubilities and levels of magma degassing affect the speciation and volume of ash-leachates (Oppenheimer, 2003), which are largely governed by the composition of the source magma (Armienta et al., 2002). Additional factors are also important, such as tephra particle size, gas:ash ratios, and the time spent in the volcanic cloud (Oskarsson, 1980; Witham et al., 2005). Adsorption of volatiles is variable, with SO_4^{2-}, Cl and F showing preferential enrichment on tephra surfaces (Delmelle et al., 2000, 2007). Up to 40% of sulfur species and 10–20% of HCl can be scavenged by tephra in the eruption column

* Corresponding author. Present address: School of Ocean and Earth Sciences, University of Southampton, National Oceanography Centre, European Way, Southampton SO14 3ZH, UK. Fax: +44 0 23 8059 3052.
E-mail address: m.jones@noc.soton.ac.uk (M.T. Jones).

0016-7037/$ - see front matter © 2008 Elsevier Ltd. All rights reserved.
doi:10.1016/j.gca.2008.05.030

and volcanic cloud (Rose, 1977; Varekamp et al., 1984). Adsorbed volatiles can leach host particles prior to deposition and alter dissolution rates upon mixing with surface water (Wolff-Boenisch et al., 2004a). Smaller particles are better scavengers of volatiles due to their higher surface area:mass ratio (Rose, 1977; Oskarsson, 1980). This allows more efficient heat transfer between the particle and the atmosphere, encouraging preferential condensation of soluble elements on fine tephra surfaces in the volcanic cloud.

The deposition of unhydrated, or 'pristine', tephra into aqueous environments will instigate the dissolution of soluble accumulations on particle surfaces. Dissolution of volcanic glass occurs at rates several orders of magnitude lower than ash-leachate dissolution (Gislason and Eugster, 1987; Gislason and Oelkers, 2003; Wolff-Boenisch et al., 2004b). Therefore, the initial chemical fluxes into solution will be dominated by the release of ash-leachates. The rapid release of nutrients and metals following the mixing of unhydrated ash or aerosols with surface waters has been the focus of field studies (Gislason et al., 2002; Uematsu et al., 2004; Flaathen and Gislason, 2007), and experimental studies (Frogner et al., 2001; Duggen et al., 2007). The experimental studies add weight to the hypothesis that deposition of tephra can instigate a rise in marine primary productivity, representing an increased biological pump for atmospheric CO_2 (Sarmiento, 1993; Watson, 1997; Frogner et al., 2001; Duggen et al., 2007). Evidence for phytoplankton blooms as a result of volcanogenic sedimentation have been observed in lakes (Smith and White, 1985) and in oceans, based on preliminary satellite data (Duggen et al., 2007). Bio-incubation experiments have shown diatoms utilizing nutrients from volcanic ash (Duggen et al., 2007). Mesoscale iron enrichment experiments have shown that Fe addition to low chlorophyll ocean waters can instigate elevated marine primary productivity (Martin et al., 1994; Boyd et al., 2000).

The experimental investigations suggest that pristine volcanic ash could cause widespread changes in nutrient availability in surface waters, but the conclusions are based on a relatively small sample set and use a variety of experimental techniques. In this study we assess the fluxes and chemical variation of ash-leachate dissolution from volcanic ash samples of varying compositions and ages. We use one sample from Iceland and several samples from volcanoes around the Pacific and Caribbean. The aim of testing a range of ash samples is to assess how volcanoes of differing provenances affect nutrient release, as well as providing an indicator for the reduction in ash-leachate availability from unhydrated ash over time. Three water samples are used as solvents in the experiments, allowing variations in ash-leachate release as a function of background nutrient levels and buffering capacities to be assessed. Attempts are made to quantify the relative fluxes of bulk dissolution rates and soluble surface accumulations to assess the relative importance of ash-leachate release against glass dissolution for volcanic sedimentation into surface waters. Finally, mixing ratios of ash and surface waters are estimated to assess the fertilization and toxicity potential of ash-leachates.

2. MATERIALS AND METHODS

2.1. Ash sample collection

Eight samples were used from seven volcanoes of varying ages, eruption type, and silica contents (Fig. 1). The bulk chemical compositions of these ash samples are shown in Table 1. We use the same sample of ash from the 2000 eruption of Hekla, Iceland, as used by Frogner et al. (2001). Hekla is an unusual composition, with a combined hotspot and constructive plate margin magma source, coupled with high fluorine in the eruptive products (Oskarsson, 1980; Moune et al., 2006). The sampling is described in Frogner et al. (2001). Since collection, the ash has since been stored first in a freezer at −18 °C, then in a desiccator from 2005 after freeze-drying. Approximately 5% of the collected sample was interstitial snow, as the eruption occurred during a snowstorm. Snow particles are efficient scavengers of aerosol particles (Graedel and Franey, 1975), which will have led to some enrichment of ash-leachates on tephra surfaces during the freeze-drying process. While this may lead to an overestimation of ash-leachates adsorbed to Hekla ash, the expected degree of contamination is low as the sample was collected prior to the main phase of precipitation. The increased deposition of aerosols through snowfall is also a likely contributor for many high-latitude eruptions, implying that the Hekla 2000 sample can be treated as representative of similar eruptions.

The most recent ash sample is from a vulcanian summit explosion of Galeras, Colombia, in 2005. Ash was collected by Gloria Cortés of the Ingeominas Volcanic Observatory. Ash from the 2003 dome collapse eruption of the Soufrière Hills volcano on Montserrat was provided by Sue Loughlin at the Montserrat Volcanic Observatory. Two samples were provided by Bill Rose of Michigan Technological University from two historic eruptions of Santiaguito, a vent on the side of Santa Maria volcano, Guatemala. The 1998 sample is elutriated ash associated with a block and ash flow from a dome collapse. A much older Santiaguito sample was also provided from a small vertical explosion in 1968, analogous to more recent observations at the volcano (Bluth and Rose, 2004). Older ash samples of a 1994 eruption of Sakura-jima (Japan) and the 1980 eruption of Mount St. Helens (USA) were donated by Claire Horwell of Durham University. The final sample used is from the 1993 eruption of Lascar (Chile), collected from the top of the pyroclastic deposits by M.T. Jones in 2004. This sample is not pristine, though the exceptionally dry conditions of the Atacama Desert may have allowed some of the ash-leachates to be preserved.

2.2. Seawater sample types and collection

The experiments were conducted using de-ionized (DI) water (18 MΩ) and two seawater samples from contrasting surface water environments. The first sample is from a nutrient rich coastal area in the North Atlantic, south of Iceland's Reykjanes peninsula (63°N, 21.5°W; Fig. 1). The sample was collected in June 1999. The second sample was collected from the Southern Ocean in April 2004, east

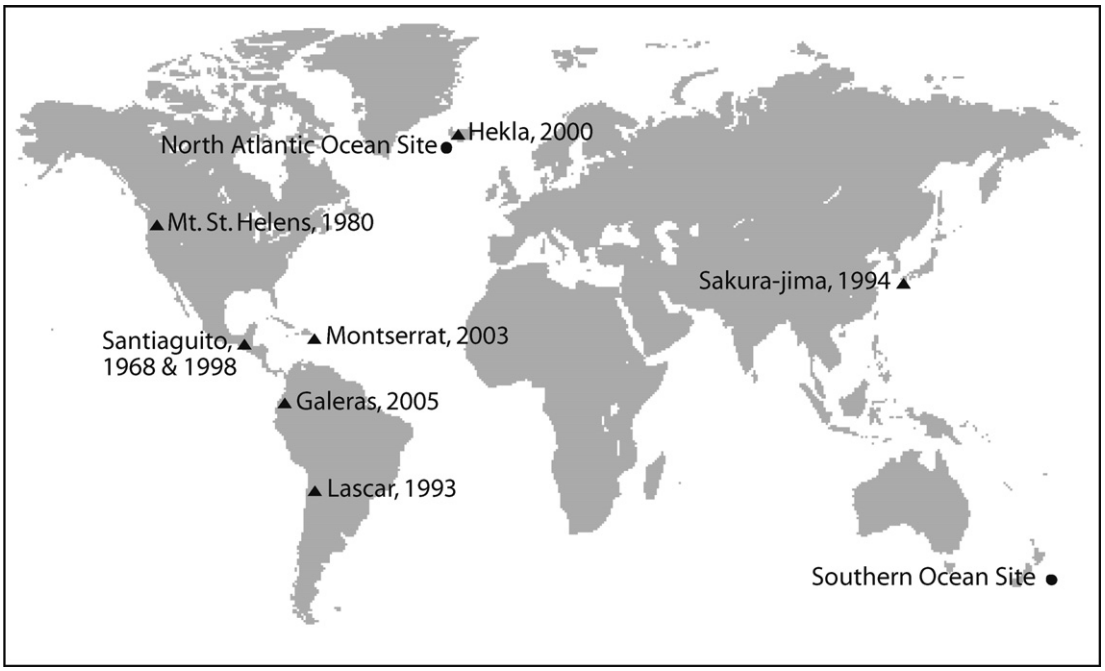

Fig. 1. Sample volcanoes with the year(s) of eruption (triangles), and sites where surface ocean water was sampled (circles).

of New Zealand's South Island (43 °30′S, 178°E; Fig. 1). Both seawater samples were filtered through a 0.2 μm cellulose acetate filter and then radiated for 4 h with ultraviolet light to remove particulate matter and kill any remaining biota. The seawater samples were then stored in the dark before being used in the experiments. The Atlantic Ocean sample has a pH of 7.95 at 20.2 °C, with an alkalinity of 2.04 meq./l. The Southern Ocean sample has a pH of 7.75 at 20.5 °C, with a measured alkalinity of 1.96 meq./l. The pH was measured by glass combination electrode at laboratory temperatures recorded in electronic annexes EA-1 and EA-2. The pH buffers and unknown solutions were at the same temperature. The pH meter was calibrated against certified pH buffers (Titrisol/Merk) cover the pH range of the solutions measured. The analytical error was ±0.05 pH units. Background salinity and nutrient concentrations are shown in EA-2 and in Stefánsdóttir and Gislason (2005).

2.3. Experimental methods

To allow direct comparisons with previous work, we have attempted to apply the same methods as used in Frogner et al. (2001). The ash samples were dry sieved with nylon sieves to between 45 and 125 μm. The experiments were conducted in Teflon single pass plug flow-through reactors with an inner diameter of 8 mm and a length of 200 mm. A thermostatic water bath kept the temperature of the reactor constant at 25 ± 0.2 °C. The plug flow-through reactors had 45 μm nylon sieves at each end, with an additional 0.2 μm cellulose acetate membrane filter at the end of the apparatus to ensure that the samples were not contaminated with particulate matter. At the beginning of each experiment, 5 g of ash was placed as a stationary bed in a plug flow-through reactor. Water was then continuously pumped through at a flow rate of 60 ± 5 ml h^{-1}, simulating the settling of ash through the water column. The settling of ash through the euphotic zone is poorly constrained, so we set our flow rate to that used by Frogner et al. (2001). Subaqueous settling rates for aggregated volcanic ash have been estimated to be in excess of 1670 m/day (Wiesner et al., 1995). Settling rates for single ash particles are therefore less rapid due to high particle vesicularity and maintained suspension of smaller particles. Ash deposition rates can also affect settling rates by changing convective sedimentation (Carey, 1997).

Initial experiments were conducted using de-ionized (DI) water and ran for 8 h. Due to a limited supply of ash from older eruptions, only the four most recent samples (Galeras, Montserrat, Hekla, and Santiaguito) had enough material to perform seawater experiments, which ran for 24 h. Fifty milliliters were analyzed, 40 ml for inductively coupled plasma—atomic emission spectroscopy (ICP-AES) analysis, 5 ml for pH measurements and 5 ml for ion chromatography (IC) analysis. The 40 ml samples were immediately acidified to 1% by volume with Suprapure HNO_3, then stored in acid cleaned polythene bottles. Speciation and saturation state calculations were conducted using the PHREEQC program (Parkhurst and Appelo, 1999). The majority of element concentrations were ascertained using ICP-AES analysis, while ion chromatography was used to quantify NO_2^-, NO_3^-, F, Cl, and SO_4^{2-}. NH_4^+ was determined using the Automated Phenate titration method in DI water, described in Standard Methods for the examination of water and wastewater, American Water Works Association (AWWA), 2005. Samples were fed manually to prevent ammonia concentrations increasing in the auto-sampler, but otherwise the method is the

Table 1
Summary of bulk ash sample compositions using X-ray fluorescence (XRF) spectrometry

	Galeras	Montserrat	Hekla	Santiaguito	Sakura-jima	Lascar	Mount St. Helens	Santiaguito
Classification	Andesite	Andesite	Basaltic-Andesite	Andesite	Andesite	Dacite	Dacite	Dacite
Eruption style	Vulcanian	Dome collapse	Sub-plinain	Dome collapse	Vulcanian	Sub-plinain	Plinian	Strombolian
Eruption date	24th Nov 2005	12th July 2003	26th Feb 2000	30th Nov 1998	1st Jan 1994	19th April 1993	18th May 1980	Sept. 1968
Collection date	24th Nov 2005	12th July 2003	26th Feb 2000	30th Nov 1998	4th Jan 1994	10th Nov 2004	18th May 1980	Sept. 1968
Sample site	Pasto (9 km)	Olveston (4 km)	11 km NNW	Unknown	Arimura (2.7 km)	7 km NW	Spokane (378 km)	Unknown
SiO_2	57.03	61.91	54.80	62.63	59.10	60.20	64.97	63.45
TiO_2	0.72	0.56	1.98	0.45	0.78	0.84	0.65	0.47
AI_2O_3	17.44	16.37	14.35	18.08	15.95	16.20	16.07	16.94
Fe_2O_3	7.47	6.57	4.38	4.51	7.96	6.00	4.44	2.27
FeO	Ψ	Ψ	7.48	Ψ	Ψ	Ψ	Ψ	2.56
MnO	0.08	0.15	0.27	0.15	0.16	0.11	0.06	0.12
MgO	2.11	2.34	2.81	1.60	3.69	3.91	1.54	1.87
CaO	5.66	6.33	6.65	5.27	6.94	6.91	4.49	5.03
Na_2O	2.93	3.86	4.01	4.75	3.40	3.54	4.81	4.91
K_2O	1.64	0.92	1.27	1.55	1.44	1.72	1.37	1.59
P_2O_5	0.21	0.15	0.96	0.21	0.15	0.25	0.18	0.19
LOI	4.36	0.46	−0.43	0.44	0.11	0.22	0.98	Not known
Total	99.91	99.63	98.96	99.79	99.68	99.68	99.56	99.73

The Galeras and Santiaguito samples were done in this study, other results were collated from previous investigations (Calvache and Williams, 1997; Smith et al., 1982; Risacher and Alonso, 2001; Wolff-Boenisch et al., 2004b; Horwell et al., 2007). Eruption type and collection information is shown, where known. Ψ, No data for partitioning between FeO and Fe_2O_3.

same as the standard procedure. The ionic load of seawater prevented ammonium analysis by this titration method, and the sensitivity of the IC machine is an order of magnitude higher than the maximum NH_4^+ measured in the DI water in these experiments. The maximum time lag between sampling and analysis was three weeks.

The concentrations of elements are measured in moles per liter, while the fluxes are standardized to moles per gram of ash per hour. When comparing the fluxes from Hekla ash in this study to the dissolution of Hekla glass in Wolff-Boenisch et al. (2004b), we re-standardize the results to geometric surface area (A_{geo}). This is calculated by Brantley et al. (1999) and Gautier et al. (2001):

$$A_{geo} = \frac{6}{\rho \cdot d_{eff}} \quad (1)$$

with ρ representing the volcanic glass density, the number 6 is based on the assumption of a spherical glass particle shape, and d_{eff} is the effective particle diameter. This is obtained from Tester et al. (1994):

$$d_{eff} = \frac{d_{max} - d_{min}}{\ln\left(\frac{d_{max}}{d_{min}}\right)} \quad (2)$$

where d_{max} and d_{min} are the maximum and minimum particle sizes used in the experiments, assuming a homogenous particle distribution.

2.4. Ash sample characterization

The ash samples vary from Basaltic-Andesite to low Si Dacite (Fig. 2). Although each sample is sieved, there is a large variation in particle size fraction and therefore particle surface area per gram. Fig. 3 shows Scanning Electron Microscope (SEM) images of the four most recent ash samples after contact with DI water. The Galeras and Santiaguito samples have some particles smaller than 45 μm, suggesting that these have become detached from host particles or accretionary lapilli during the experiments. The Galeras sample is characterized by cristobalite and occasional euhedral crystals of gypsum, with rare volcanic glass. Accretions of salts and sulfides as lapilli or adhered to particle surfaces are extremely abundant. The source of the gypsum is most likely to be reworked country rock evaporite deposits incorporated into the eruptive products (Calvache and Williams, 1997). This concurs with a large loss on ignition observed when calculating the bulk rock composition (Table 1). The Montserrat sample is more crystalline, with dominant cristobalite, pyroxene, and minor amounts of volcanic glass (Fig. 3). Hekla ash differs significantly from the other samples, with comparatively low Si levels and high Fe and P (Fig. 2, Table 1). Over 60% of particles are glass, with plagioclase and pyroxene the dominant crystals. The glass particles are highly vesicular, as shown in Fig. 3. Santiaguito ash is dominated by cristobalite and plagioclase crystals, with abundant smaller glass fragments.

2.5. Experimental and computational uncertainties

Uncertainties associated with ascertaining element release rates in water arise from various sources, including the measurement of aqueous solution concentrations, fluid flow rates, and ash-leachate degradation or removal prior to analysis. Uncertainties of element fluxes increase for more dilute concentrations, especially when mixed with ocean surface water due to the high ionic loading. Standard fluid flow rates were occasionally hampered by blockages in the apparatus, leading to errors in the flow rate. The total errors for sample concentrations do not exceed ±10%.

There may be important differences between the experimental set up and the response to mixing of ash with water in natural environments. Many reactions are temperature

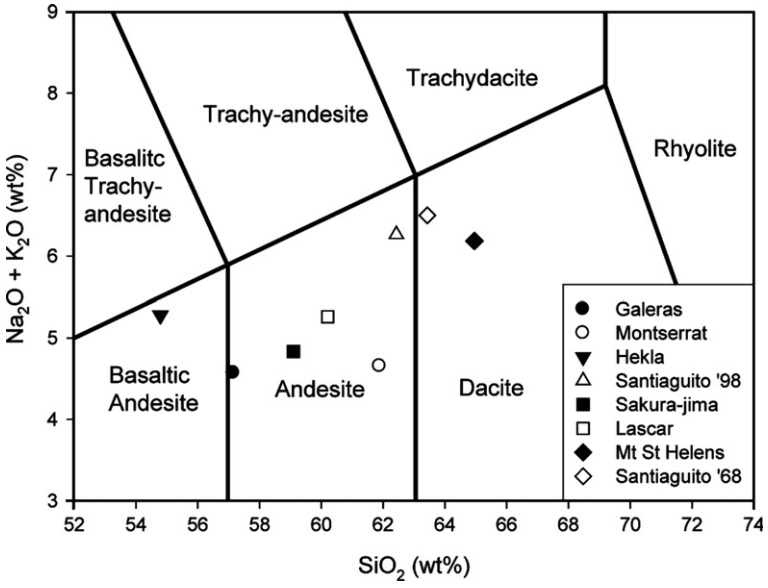

Fig. 2. Classification of samples based on volcanic ash silica content and alkali metal concentrations (Le Bas et al., 1991). Samples range from Basaltic-Andesite to low Si Dacite.

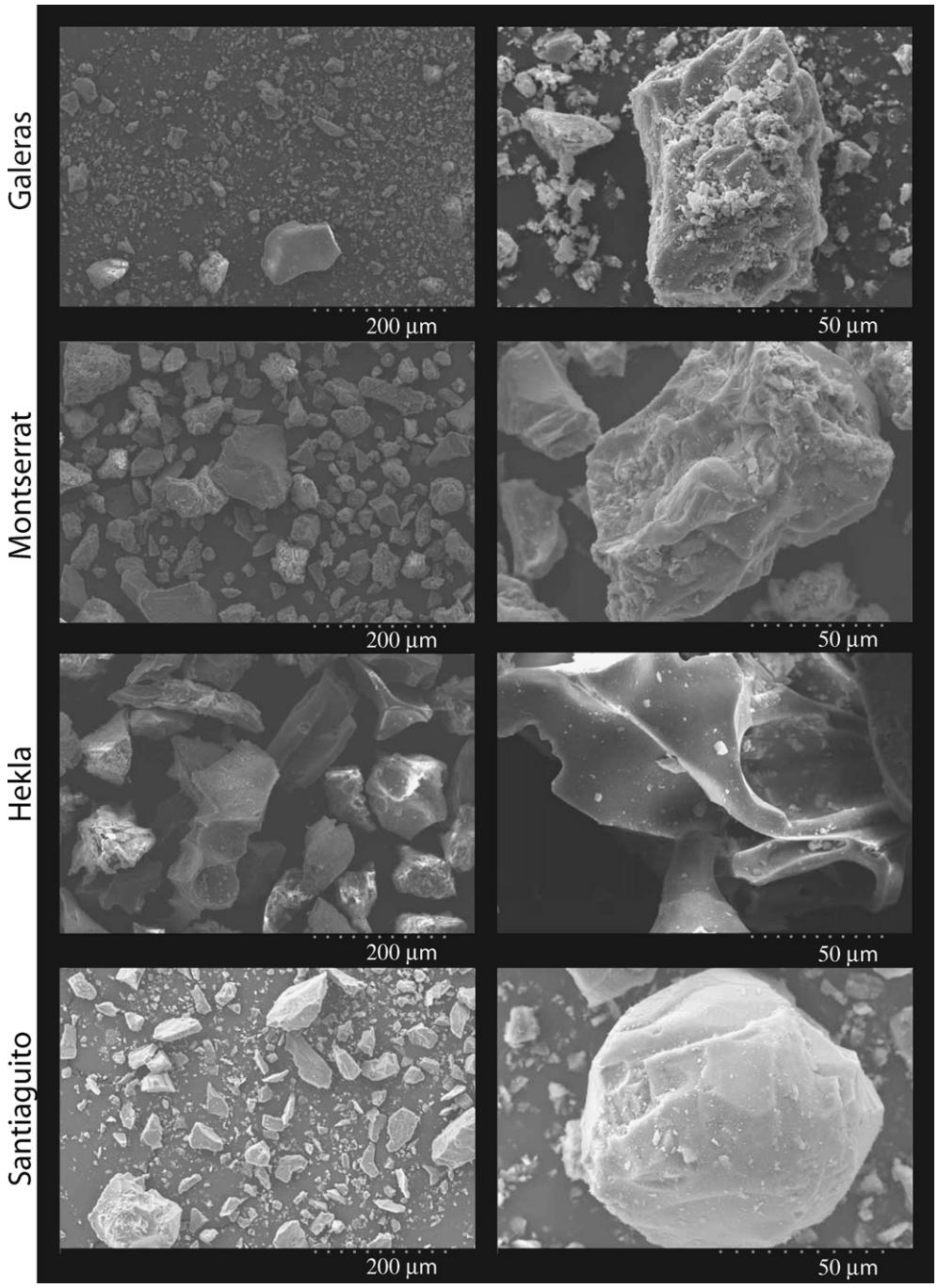

Fig. 3. SEM images of ash samples after contact with de-ionized water. The left-hand column shows the ash sample at 200× magnification. The right hand column shows typical particles at 800× magnification. Though all samples were sieved to between 45 and 125 µm, there is significant fine material present in the Galeras and Santiaguito samples. These are inferred to have been present as accretionary lapilli or stuck to larger host particles prior to contact with water, which were then released due to breakdown of the cement.

dependent, so fluxes and ash-leachate speciation could vary with water temperature. Therefore, our experiments may not accurately mimic deposition of volcanic ash into cold water environments. The ratio of ash to water affects ash-leachate release and concentrations (Witham et al., 2005). Low ash:water ratios, or rapid diffusion of leached anions, could negate any pH change and alter nutrient fluxes.

3. RESULTS

3.1. General observations

The results from the DI water and seawater experiments are summarized in EA-1 and EA-2, respectively. The greatest initial concentrations are in DI water, with

SO_4^{2-} ($\leqslant$16.7 mmol l^{-1}), Ca ($\leqslant$15.4 mmol l^{-1}), Cl ($\leqslant$7.2 mmol l^{-1}), F ($\leqslant$7.1 mmol l^{-1}), Na ($\leqslant$7 mmol l^{-1}), Al ($\leqslant$2.2 mmol l^{-1}), and Mg ($\leqslant$2 mmol l^{-1}) showing the highest fluxes at the 60 ml h^{-1} flow rate. The total amounts of components released during the first 8 h in DI water for all samples are shown in Table 2. Selected comparisons between element release in DI water and the two seawater samples are shown in Table 3 for the younger samples, namely Galeras, Montserrat, Hekla, and Santiaguito (1998). Na, Mg, Cl, K, and Br fluxes were unobtainable in seawater due to the high ionic load and high background concentrations. Ca, F, SO_4^{2-}, and several minor constituents have fluxes too low to be detected due to the increase in detection limit associated with the ionic loading. Only initial dissolution rates from the samples rich in soluble material are distinguishable in these cases. For example, background levels of fluorine in natural seawater were measured at 49–71 μmol l^{-1}, much lower than the elevated concentrations from contact with Hekla ash (0.2–5.2 mmol l^{-1}) at the 60 ml h^{-1} flow rate. Initial fluxes from the Galeras samples are recognizable above background values for 6–7 h. The initial concentrations from the other ash samples are about 10 μmol l^{-1}, too low to distinguish from background seawater concentrations.

Initial contact of volcanic ash with DI water results in an initial reduction in pH, which increases as each experiment progresses (Fig. 4). The Hekla ash sample shows the greatest change, initially dropping to pH 3.5 and staying below pH 4.7 throughout the experiment. In comparison, pH changes caused by Galeras, Montserrat, and Sakura-jima are less severe, with pH decreasing to 4.6 initially and returning to around pH 6 after 8 h. There is little change in pH during the experiments using ash from Mount St. Helens, Lascar, and both samples from Santiaguito. The change in pH in the seawater experiments is shown in Fig. 5. The reactions show initially low pH conditions, though the decrease in pH is much more transient. The charge balances ($100 \times [\text{Cations} - |\text{Anions}|]/[\text{Cations} + |\text{Anions}|]$) of the reactant solutions was obtained using PHREEQC. All solutions show charge balances of ±3%,

Table 2
Total fluxes of elements released from volcanic ash mixed with de-ionized water within 8 h

	(μmol/g)	Galeras	Montserrat	Hekla	Santiaguito 98	Sakura-jima	Lascar	Mount St. Helens	Santiaguito 68
Volatile	F	9.0	0.3	165.3	0.2	0.3	0.1	0.4	0.4
	Cl	50.2	49.9	92.9	5.8	3.7	2.0	9.3	5.0
	Br	0.07	0.09	0.06	0.03	0.00	0.00	0.04	0.03
	SO_4^{2-}	554.2	12.5	8.1	3.8	1.0	1.7	1.0	8.5
Alkali metals	Li	0.18	0.04	0.07	0.02	0.00	0.01	0.00	0.02
	Na	46.9	26.4	84.3	7.7	1.9	1.5	1.8	6.1
	K	4.0	1.3	5.4	0.4	0.2	0.1	0.2	0.7
Alkali earths	Mg	28.5	11.1	9.9	0.4	0.2	0.1	0.4	0.7
	Ca	588.6	12.8	32.7	2.1	0.6	2.1	1.9	5.4
	Sr	0.40	0.01	0.08	0.01	0.00	0.01	0.00	0.01
	Ba	0.005	0.000	0.035	0.001	0.000	0.001	0.000	0.011
Other major elements	B	0.53	0.36	0.31	0.13	0.00	0.04	0.02	0.09
	NO_3^-	0.3	6.5	13.3	0.0	0.1	0.0	0.0	0.0
	NO_2^-	0.4	4.5	6.4	0.0	0.0	0.0	0.0	0.0
	NH_4^+	0.4	0.6	0.3	*No data*	0.6	*No data*	*No data*	*No data*
	Al	6.1	0.3	33.7	0.3	0.2	0.1	0.1	0.0
	Si	0.8	0.5	13.9	0.8	0.2	0.4	0.3	0.4
	P	0.02	0.02	2.18	0.09	0.01	0.06	0.13	0.23
Minor elements	Ti	0.00	0.00	0.39	0.00	0.00	0.00	0.00	0.00
	V	*b.d.l.*	*b.d.l.*	0.004	0.001	*b.d.l.*	0.003	0.000	0.000
	Cr	0.001	0.004	0.002	0.004	0.006	0.003	0.004	0.010
	Mn	0.71	0.72	0.67	0.02	0.00	0.00	0.01	0.03
	Fe	0.12	0.04	10.85	0.01	0.03	0.01	0.04	0.03
	Co	0.022	0.005	0.005	0.001	0.000	0.000	0.001	0.001
	Ni	0.026	0.009	0.009	0.005	0.004	0.002	0.014	0.005
	Cu	0.031	0.043	0.011	0.001	0.018	0.004	0.003	0.005
	Zn	0.08	0.05	0.10	0.00	0.04	0.01	0.05	0.03
	As	0.001	0.000	0.001	0.001	0.001	0.001	0.001	0.002
	Se	0.002	0.001	0.001	0.002	0.002	0.001	0.001	0.002
	Mo	0.000	0.000	0.000	0.000	*b.d.l.*	*b.d.l.*	0.000	0.000
	Cd	0.001	0.000	0.003	0.000	0.000	0.000	0.000	0.000
	Sn	0.001	0.001	0.001	0.001	0.001	0.001	0.001	0.001
	Pb	*b.d.l.*	0.001	*b.d.l.*	0.001	0.000	0.001	0.001	0.001

Fluxes are shown in μmol $g^{-1}_{(ash)}$. Values above the detection limit but below 3 significant figures are shown as 0.000, while values below detection are labeled '*b.d.l.*'.

Table 3
Comparisons of total fluxes of elements released in de-ionized water and two surface ocean water samples within 8 h

Comp. (μmol/g)	Galeras			Montserrat			Hekla			Santiaguito '98		
	DI	Atlantic	Southern	DI	Atlantic	Southern	DI	Atlantic	Southern	DI	Atlantic	Southern
F	**9.0**	4.6	5.5	**0.3**	0.6	−0.1	**165.3**	155.6	152.6	**0.2**	−0.1	−0.1
SO_4^{2-}	**554.2**	381.8	579.6	**12.5**	71.2	84.2	**8.1**	63.4	71.0	**3.8**	31.0	56.9
Li	**0.18**	0.17	0.14	**0.04**	−0.03	0.00	**0.07**	0.14	0.12	**0.02**	−0.01	−0.02
Ca	**588.6**	415.1	408.6	**12.8**	1.6	49.5	**32.7**	22.1	14.1	**2.1**	1.4	11.9
Sr	**0.40**	0.43	0.22	**0.01**	−0.04	−0.04	**0.08**	0.32	0.14	**0.01**	−0.03	−0.19
Ba	**0.005**	0.027	0.033	**0.000**	−0.001	−0.001	**0.035**	0.037	0.043	**0.001**	0.049	0.052
B	**0.53**	0.43	0.19	**0.36**	0.45	0.55	**0.31**	1.23	0.92	**0.13**	0.22	0.06
Al	**6.1**	0.7	0.5	**0.3**	0.2	0.2	**33.7**	16.1	19.7	**0.3**	0.1	0.1
Si	**0.8**	0.1	0.4	**0.5**	0.4	0.7	**13.9**	13.8	17.2	**0.8**	0.3	0.5
P	**0.02**	−0.01	0.00	**0.02**	−0.01	0.03	**2.18**	0.37	0.36	**0.09**	0.02	0.02
Ti	**0.00**	0.00	0.00	**0.00**	0.00	0.00	**0.39**	0.15	0.19	**0.00**	0.00	0.00
Mn	**0.71**	0.58	0.71	**0.72**	0.54	0.53	**0.67**	0.72	0.92	**0.02**	0.05	0.05
Fe	**0.12**	0.05	0.01	**0.04**	0.10	0.02	**10.85**	7.09	8.92	**0.01**	0.02	0.04
Co	**0.022**	0.017	0.019	**0.005**	0.004	0.004	**0.005**	0.005	0.006	**0.001**	0.000	0.001
Ni	**0.026**	0.020	0.021	**0.008**	0.003	0.003	**0.009**	0.013	0.002	**0.005**	0.001	0.002
Cu	**0.031**	0.014	0.013	**0.043**	0.011	0.007	**0.011**	0.007	0.009	0.002	**0.002**	0.003
Zn	**0.08**	0.06	0.04	**0.05**	0.03	0.02	**0.10**	0.08	0.09	**0.00**	0.00	0.00

The seawater fluxes are the concentrations after contact with ash minus the background measured concentrations. Negative values are where concentrations have decreased after contact with ash (e.g., P). Fluxes are shown in μmol $g^{-1}_{(ash)}$.

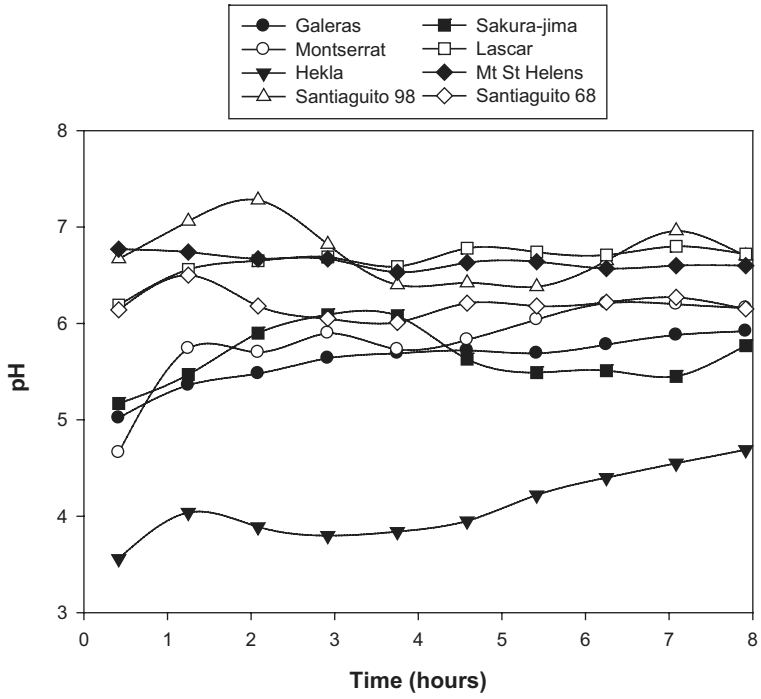

Fig. 4. Illustration showing pH changes in the experiments mixing volcanic ash with de-ionized water at 25 °C. The pH measurements were done at between 20.5 and 22.2 °C.

except for the first DI water sample reacted with Hekla ash, which has a charge balance of +17.4%. Initial acidification is comparable to the response in DI water, with Hekla causing a greater decrease in pH than the three subduction zone samples. The high buffering capacity of the seawater curtails the drop in pH, limiting elevated dissolution for acidity dependent reactions. Buffering in these experiments will be slower than in nature, as the water in contact with the ash is restricted to 60 ml h^{-1}.

3.2. Volatile release

The releases of volatiles can affect glass dissolution rates in solvents (Wolff-Boenisch et al., 2004a) and the fluxes of

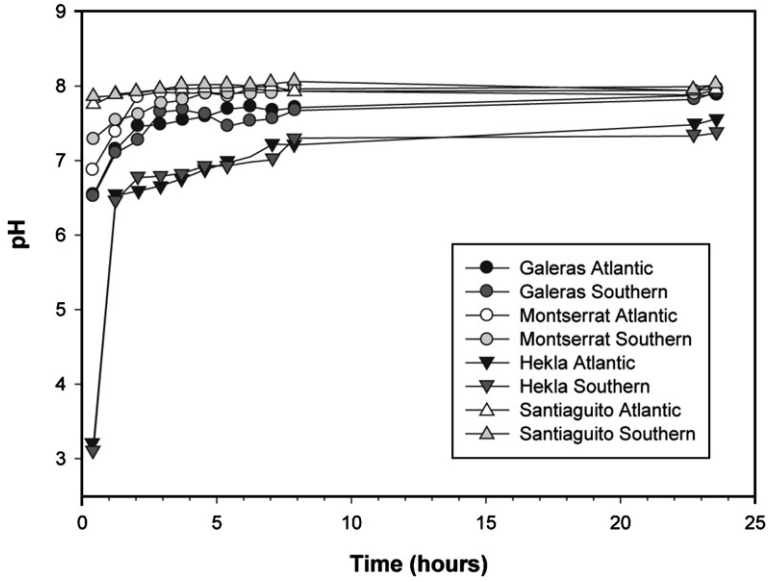

Fig. 5. pH changes in the experiments mixing volcanic ash with surface water samples from the North Atlantic and Southern Oceans at 25 °C. Temperatures of samples when pH was measured were between 20.5 and 22.1 °C. Black and white labels show North Atlantic sample water, grayscale points show Southern Ocean water.

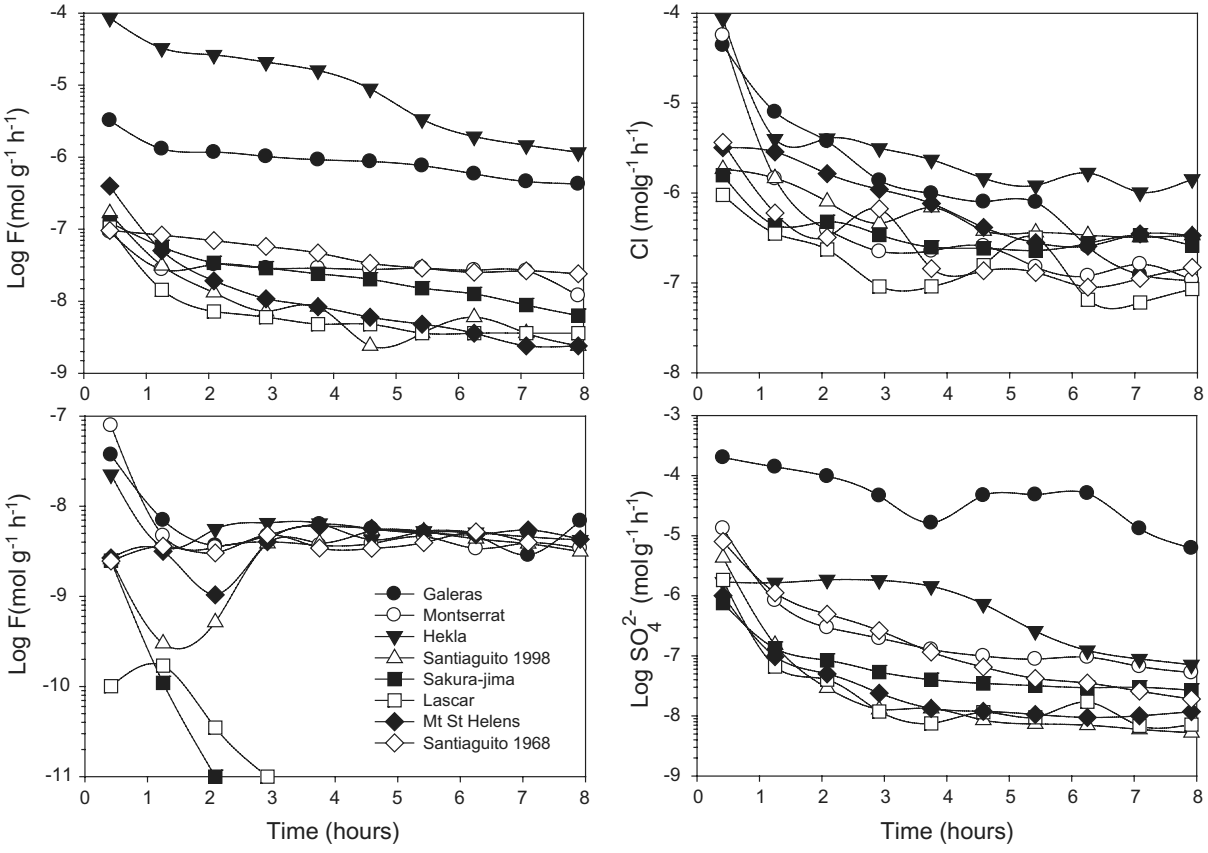

Fig. 6. Fluxes of halogens and sulfate from volcanic ash in de-ionized water at 25 °C. Fluxes are shown in mol $g_{(ash)}{}^{-1}\,h^{-1}$. Analytical errors are commonly <10%.

these elements vary by the greatest margin between each sample. Halogen and sulfate fluxes in DI water are shown in Fig. 6. The rates and quantities of elemental release differ for each ash sample. In particular, the F flux from the Hekla ash is far greater than any other sample. Aqueous concentrations of F initially reach 7.14 mmol l^{-1} at the 60 ml l^{-1} flow rate in DI water, which equates to 85 μmol $g^{-1}_{(ash)}$ h^{-1}. This is over 25 times more than the highest flux from a subduction zone ash sample (Galeras) and nearly 800 times more than the lowest flux (Santiaguito, 1968). Initial volatile fluxes from the older ash samples are consistently lower than the recent samples from Galeras, Montserrat, and Hekla. This suggests a natural decay of surface ash-leachates, which we will focus on in Section 4.

The F fluxes from Hekla and Galeras appear to correlate well between the DI water and seawater (Table 3). For the Montserrat and Santiaguito (1998) samples, background concentrations in seawater obscure accurate comparisons between water samples. The close correlation of results from Hekla and Galeras between solvents (Table 3) implies that F fluxes measured in the other DI water experiments will be comparable in seawater. The initial Cl fluxes from the Hekla, Galeras, and Montserrat samples are comparable at between 44 and 86 μmol g^{-1} h^{-1}, which are significantly higher than the other ash samples (Fig. 6). Bromine release shows a more uniform behavior between samples, though the three youngest ash samples show the greatest initial fluxes, up to 78 nmol g^{-1} h^{-1}.

Concentrations of sulfate vary considerably between ash samples. Galeras in particular shows a very high SO_4^{2-} flux, initially 200 μmol g^{-1} h^{-1} (Fig. 6). This is an order of magnitude higher than fluxes from any of the other samples, a product of the gypsum and sulfate accretions in the tephra. Comparisons of SO_4^{2-} release appear to vary considerably with solvent composition. Galeras ash, with high available SO_4^{2-}, shows comparable fluxes between DI water and seawater. For Montserrat, Hekla, and Santiaguito however, the SO_4^{2-} flux is around a magnitude greater in seawater (Table 3). This shows a preferential removal of SO_4^{2-} from ash surfaces in alkaline conditions, unless the total SO_4^{2-} available is considerable. The likely cause is that the zero point charge (ZPC) for volcanic glass surfaces are commonly around 7, where surfaces are positively charged at lower pH and negatively charged at higher pH (Wolff-Boenisch, 2004). Thus double charged anions such as SO_4^{2-} have a strong tendency to desorb from negatively charged glass surfaces once the experimental pH is buffered to background pH values (~7.8). The ZPC of Quartz is at pH 3 (Riese, 1982), so one would expect tephra abundant in silica polymorphs like cristobalite to have different desorption behavior than glass dominated tephra.

3.3. Nutrient and Al release

The major nutrients and Al fluxes in DI water are shown in Fig. 7. The majority of nutrients are released in the first hour, typically 40–90% of the total released in 8 h. The fluxes of Al, Si, P, and Fe from Hekla ash are considerably higher than from any other sample in both DI water (Fig. 7) and seawater. In comparison, the initial fluxes of Mn and Zn are comparable for Galeras, Montserrat, and Hekla. There is no discernable difference in Al and Si release rates between DI water and seawater when the fluxes are high, as with Hekla. However, the smaller fluxes from the three subduction zone volcanoes show reduced Al and Si release rates in seawater (Table 3). Many key micronutrients, including Mn, Fe, Co, Ni, Cu, and Zn, show comparably high initial release rates in all solvents, suggesting that the dominant source of these transition metals are highly soluble surface metal salts.

Nitrogen was detected as nitrate, nitrite and ammonium in the reacted DI water samples. The Hekla sample showed the highest fluxes of NO_3^- and NO_2^-, maintaining constant high fluxes for the first couple of hours at around 5.0 and 1.6 μmol g^{-1} h^{-1}, respectively. The Montserrat ash was the only other sample to show significant fluxes of NO_3^- and NO_2^-, though the style of release is different. After early fluctuations, the NO_3^- flux plateaus at 1.6 μmol g^{-1} h^{-1}. The NO_2^- flux from Montserrat shows early oscillations in release rates, which begin to increase after 2 h from 0.2 to 1 μmol g^{-1} h^{-1} by the end of the experiment. The source of the nitrate and nitrite is not exhausted within the 8 h of the experiment. The fluxes of nitrate and nitrite from the other ash samples are considerably lower and often negligible in DI water (Table 2).

The release of NO_3^- and NO_2^- in seawater appears to be much lower than in DI water. NO_3^- concentrations were measured at 3.3 μmol l^{-1} in North Atlantic surface water (Stefánsdóttir and Gislason, 2005) and were undetectable in Southern Ocean surface water. While typical Southern Ocean surface waters are NO_3^- rich, the sample site is further north than the areas that are generally high in macronutrients. Background concentrations in the North Atlantic sample are high enough to add significant errors to ascertaining NO_3^- release rates. Results from the Southern Ocean samples only show significant release of NO_3^- in the first few Hekla samples (EA-2), though much less than the flux in DI water. NO_2^- fluxes are also apparently diminished in seawater, with trace fluxes in all experiments except the Hekla sample mixed with North Atlantic water. NO_2^- concentrations were measured at 1.47 μmol l^{-1} in North Atlantic surface water (Stefánsdóttir and Gislason, 2005), so it is unusual that it is undetectable in the water after contact with any subduction zone ash sample.

The measured fluxes of NH_4^+ are largely comparable between samples in DI water (Fig. 7). Unfortunately, data were only ascertained for the Galeras, Montserrat, Hekla, and Sakura-jima samples. The style of release from the four samples is characterized by a high initial flux that decreases steadily through time. The Montserrat sample shows the highest initial flux (0.3 μmol g^{-1} h^{-1}, Fig. 7) and total release (0.61 μmol g^{-1}, Table 2) of NH_4^+, while Hekla releases the least of the 4 samples (0.34 μmol g^{-1}). While our methods did not allow measurements of NH_4^+ in the seawater samples, the measured fluxes in DI water are comparable to previous measurements of release in seawater (Duggen et al., 2007).

Phosphorus shows the biggest difference in release rates with varying water composition (Fig. 8). As with Si and Fe,

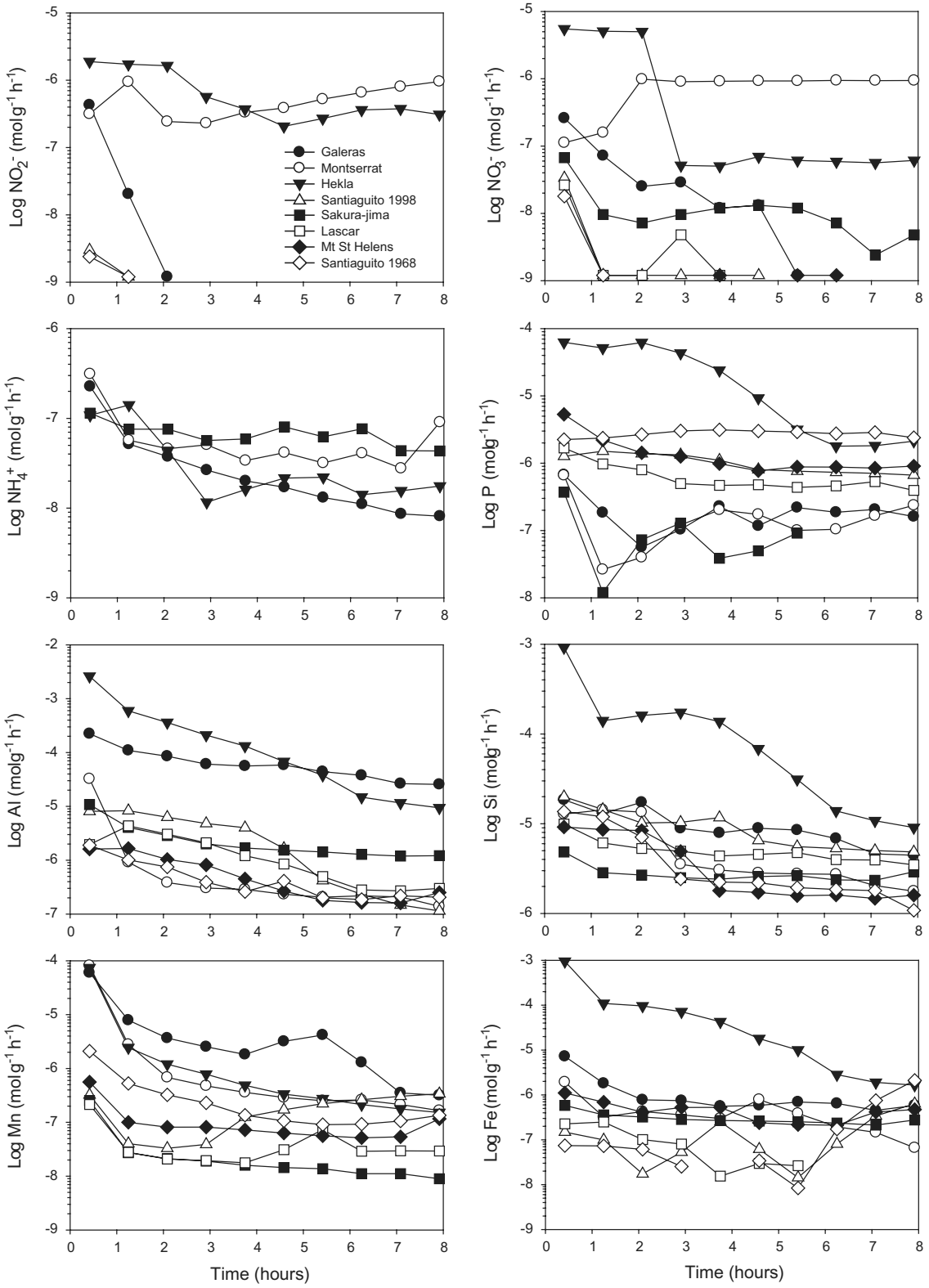

Fig. 7. Fluxes of major nutrients and aluminum from volcanic ash in de-ionized water at 25 °C. Analytical errors are commonly <10%.

the initial mobilization of P from Hekla ash in seawater is comparable to the flux observed in DI water. However, the sustained release for the first 4 h in DI water is not matched in seawater, where P release quickly becomes negligible. P fluxes from Galeras, Montserrat, and Santiaguito (1998) ash behave quite differently with varying solvent,

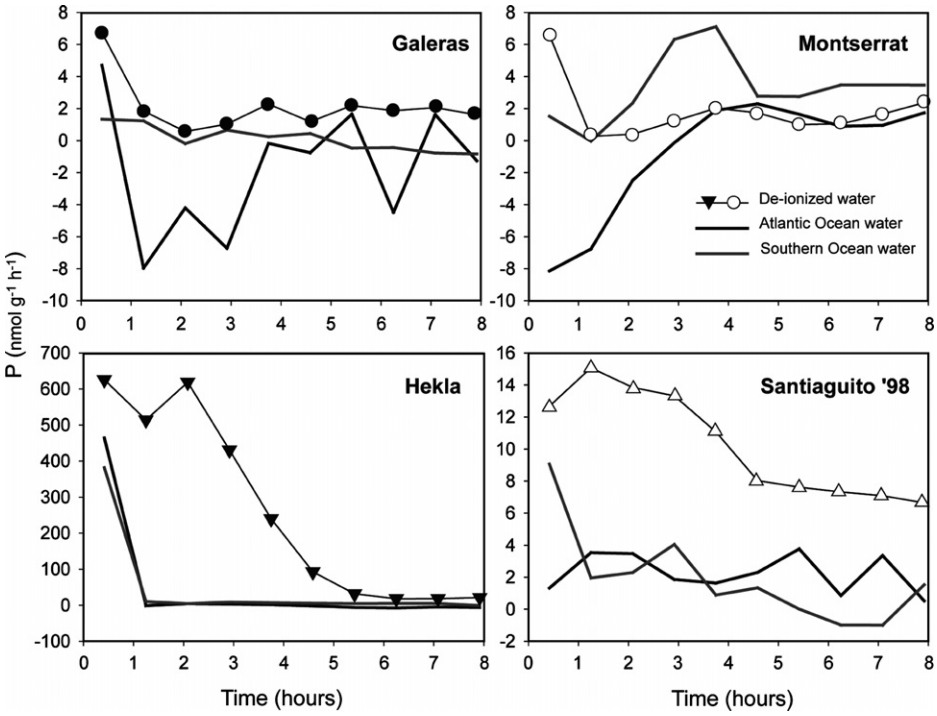

Fig. 8. Variations in phosphorus fluxes between water samples for Galeras, Montserrat, Hekla, and Santiaguito ash samples at 25 °C. The line with points is DI water using symbols from previous figures. Fluxes are in nmol g^{-1} h^{-1}.

particularly in North Atlantic surface water. There is a detectable net reduction in P concentrations in Atlantic seawater when mixed with both Galeras and Montserrat ash (Fig. 8, Table 3). Scavenging of P only occurs from Atlantic seawater as background concentrations are higher (~0.7 μmol l^{-1}) than in the Southern Ocean sample (~0.1 μmol l^{-1}). These experiments use a relatively high ash:seawater ratio (5 g:1.2 l), which may encourage re-adsorption of P. This effect may be negated in a direct release scenario in the open ocean.

4. DISCUSSION

4.1. Variations between ash and water samples

All ash samples show significant fluxes of nutrients into solution, although there are considerable variations in ash-leachate speciation and concentrations between samples. The presence of F has a large effect on the dissolution of natural glasses, increasing rates by an order of magnitude or more (Wolff-Boenisch et al., 2004a). Subduction zone volcanoes can have F rich magmas, such as Lonquimay (Chile), so the observed differences in behavior between Hekla ash and the other samples may not reflect typical differences in ash-leachate release from contrasting tectonic settings. The high F concentrations and the greater observed drop in pH in the Hekla experiments increase fluxes of important bulk magmatic elements such as Al, Si, P, and Fe. The fluxes of these elements deteriorate faster than the change in pH in DI water, suggesting that these cations are already leached from host particles and are available for immediate dissolution, rather than due to increased bulk dissolution in an F rich, acidic fluid.

The release of alkali metals and transition metals, particularly Mn, Co, Ni, Cu, and Zn, appear to show comparable fluxes independent of solvent where data are available. The hypothesis drawn from these results is that these cations are dominantly combined with halogens and sulfate as metal salts and aerosols adsorbed to particle surfaces. This is backed up by studies of trace metals in the gaseous phase at several volcanoes (Africano et al., 2002; Bernard and Le Guern, 1986; Delmelle et al., 2007). The total dissolution of these ash-leachates while in surface waters appears unaffected by large variations in acidity and alkalinity, suggesting a high solubility in these solvents. Fluxes of these elements are commonly an order of magnitude higher in the first hour than in the second, indicating that these micronutrients will be released in the upper surface waters.

The dissolution of elements that are affected by changes in pH and/or saturation states show differing styles and volumes of release with varying solvent. Al, P, and Ti are particularly affected. Elevated dissolution in acidic conditions is restricted by the high buffering capacity of seawater, resulting in greater fluxes of these elements in DI water. Al and Ti have dissolution rates that increase exponentially with lowering pH (Oelkers and Gislason, 2001), suggesting that the higher fluxes in DI water may be due to increased dissolution of glass and crystals. However, elements that have dissolution rates shown to be equally pH dependent as Al and Ti, such as Si and Fe, do not show such a difference between DI water and seawater fluxes. This suggests that the saturation states of components with respect to sec-

ondary minerals are the dominant factor in nutrient release, affecting both ash-leachate and glass dissolution.

P fluxes are the most affected by solvent composition and pH change. Andesitic ash particles scavenge P from surface waters with initially high concentrations (a negative flux); in this case North Atlantic surface water (Fig. 8). Concentrations of P in the seawater experiments are probably controlled by the saturation state of amorphous FeO(OH) in the fluid, leading to precipitation of iron-oxyhydroxide and scavenging of P to the Fe surface (Williams et al., 1976). Elevated P fluxes only occur when amorphous FeO(OH) is undersaturated in low pH conditions in the experiments, as shown in Fig. 9. pH values buffered to $\geqslant$6.5 cause the solution to become supersaturated with respect to amorphous FeO(OH). Under such conditions, dissolution of P becomes negligible and is scavenged onto Fe oxide particle surfaces. Previous studies have shown that waters that have reacted with Icelandic volcanic ash can become supersaturated with respect to various Fe and Mn oxides and oxyhydroxides at low temperatures (Flaathen and Gislason, 2007; Gislason et al., 2002). This implies that the dissolution and concentration of P and potentially other elements are likely to be extremely variable in solvents of differing pH buffering capacities, and that scavenging of P from nutrient rich surface waters is possible.

4.2. Ash-leachate decay

Comparisons of the results of this study with those obtained by Frogner et al. (2001) shows decreases in all nutrient release rates since the pioneer study on Hekla ash. Initial Fe release, for example, has decreased from 37 μmol g^{-1} h^{-1} in the initial study to 10 μmol g^{-1} h^{-1} in this study using the same Hekla ash and Atlantic surface water samples. These flux differences are well outside the range of experimental reproducibility, as measurement errors were typically $<\pm$10%. Considerable efforts have been made to maintain the pristine nature of the sample since collection (Frogner et al., 2001). The difference could stem from the variation in particle size between the two studies, which were 44–74 μm in the initial study and 45–125 μm in this analysis. Smaller particles are better scavengers of volatiles due to their higher surface area to mass ratio (Oskarsson, 1980; Rose, 1977). Volcanic glass typically has a higher fraction in smaller fragments, so it is plausible that the comparatively high surface areas of glasses compared to crystals below 74 μm could result in the differences in fluxes measured. However, SEM images do not show this to be the case for the Hekla sample (Fig. 3).

While nutrient release is highly variable between ash samples, the elemental fluxes measured in this study are broadly inversely proportional to the age of the sample. Assuming the Hekla and Galeras samples are representative of recently collected ashes, unhydrated samples greater than 10 years old tend to show diminished nutrient fluxes in comparison. Therefore, even though considerable attempts were made to maintain the pristine nature of the samples used, it appears that a natural degradation of the solubility of surface accumulations has occurred. Negligible nutrient fluxes were observed with unhydrated ash from the 1970 eruption of Hekla using the same plug flow-through reactor experiments as Frogner et al. (2001). The cause of this apparent deterioration is unclear, but has important consequences for experiments of this nature. Given the difficult nature of pristine ash collection and the age of some samples used in these and previous investigations, these findings suggest that laboratory experiments measuring ash-leachate release may underestimate the flux from tephra deposited directly into surface waters.

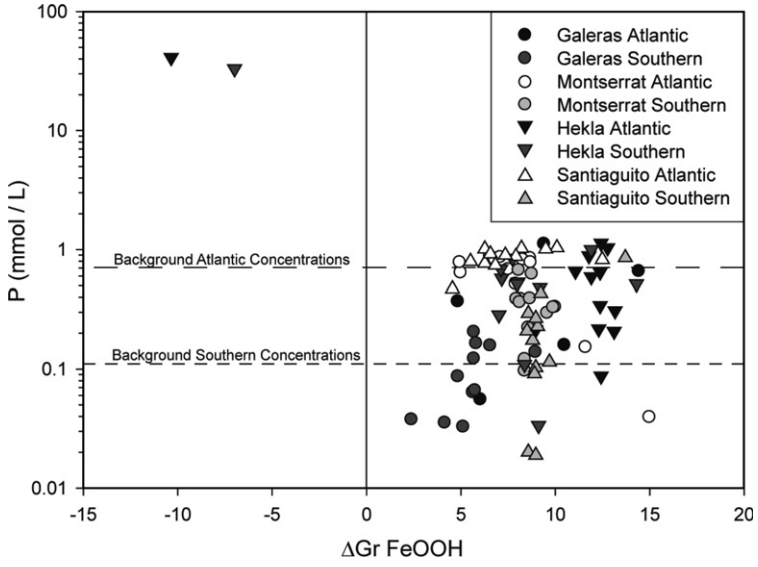

Fig. 9. Graph showing the relationship between phosphorus concentrations in water samples with amorphous FeO(OH) saturation, analyzed using the PHREEQC program. The long dashed line is the measured background concentrations in the North Atlantic, while the short dashed line represents background levels in the Southern Ocean. Black and white points show North Atlantic sample water, grayscale points denote Southern Ocean water samples.

4.3. Ash-leachate fluxes vs. bulk dissolution rates

Element fluxes are combinations of ash-leachate release and the bulk dissolution of ash particles. To assess the relative contributions of each, we focus on the release of Si and Al from the Hekla ash. A_{geo} of Hekla ash is 274.64 $cm^2\ g^{-1}$, where $\rho = 2.79\ g\ cm^{-3}$. Dissolution rates of natural glasses, including the 2000 eruption of Hekla, were analyzed by Wolff-Boenisch et al. (2004b). Dissolution of Si, normalized to A_{geo}, is 3.3×10^{-14} mol $cm^{-2}\ s^{-1}$ at pH 4.1. Al dissolution is 2.5×10^{-14} mol $cm^{-2}\ s^{-1}$ at pH 4.1 (Wolff-Boenisch et al., 2004b). These values do not incorporate the effect of F on the bulk dissolution rate, which is considerable in these solutions (Wolff-Boenisch et al., 2004a). Activities of Si and Al reach a minimum around neutral pH. In this study, dissolution rates will be higher initially due to the transient pH drop. In seawater, the recovery to background pH levels (pH ≈ 8) will dictate that dissolution rates will start high, reach a minimum and then increase again.

The initial fluxes from Hekla ash, in the present study, are far greater in all solvents than the F free bulk dissolution rates in acidic conditions. Initial release rates of Si vary from 9.3×10^{-12} to 1.3×10^{-11} mol $cm^{-2}\ s^{-1}$, while rates of Al release vary from 1.45 to 2.64×10^{-11} mol $cm^{-2}\ s^{-1}$. The bulk dissolution rate of Hekla ash in the experimental solutions using DI water, incorporating the effects of F (Wolff-Boenisch et al., 2004a), predicts elevated rates of 4.5–6.1×10^{-13} mol $cm^{-3}\ s^{-1}$ throughout the 8 h of the experiment. This is 20 times less than the initial release rate of Si and nearly 60 times less than Al release, suggesting that ash-leachates are the dominant contributor to initial element fluxes. However, after 8 h the release rates of Si and Al drop below 9.5×10^{-14} mol $cm^{-3}\ s^{-1}$, suggesting that later element fluxes are dominated by bulk dissolution of ash particles.

In seawater the transient pH drop and the high buffering capacity means the initial bulk dissolution rates will be very different to later rates. Using PHREEQC, the activities of H^+ in reacted seawater are initially an order of magnitude higher than in DI water, while approximately 3 orders of magnitude lower after 8 h. This is integral to the bulk dissolution rate (Wolff-Boenisch et al., 2004a), and initially the predicted bulk dissolution rates are between 60 and 90% of the measured fluxes of Si and Al into seawater (1–1.8×10^{-11} mol $cm^{-2}\ s^{-1}$). Bulk dissolution rates quickly drop to 10^{-15} mol $cm^{-2}\ s^{-1}$ in seawater, making the contribution of tephra dissolution negligible after buffering. The chemical fractionation of Si and Al between fluid and glass in the measured samples is shown in Fig. 10. The majority of the total liberated Si and Al is released within 50 min of contact with water. $Al_{(aqueous)}$:$Al_{(glass)}$ ratios show slightly elevated fluxes into solution for up to 4 h in the DI water experiment, allowing an additional 47–58% of Al to be released (Table 3). Si release is similar between solvents, though there is less Si released in seawater initially. The similarity between fluxes in DI water and seawater do not reflect the predicted differences in initial bulk dissolution rates between solvents. A possibility for this discrepancy, assuming that the initial release of ash-leachates is relatively uniform between solvents, is that the reacting seawater may buffer the activity of H^+ in under an hour, thereby curtailing the period of enhanced bulk dissolution. However, the most likely explanation is that the F adsorbed to particle surfaces has leached Si and Al prior to contact with water, reducing the availability of reactive surfaces and reducing the impact of solvent variance once the particles are affected by aqueous dissolution.

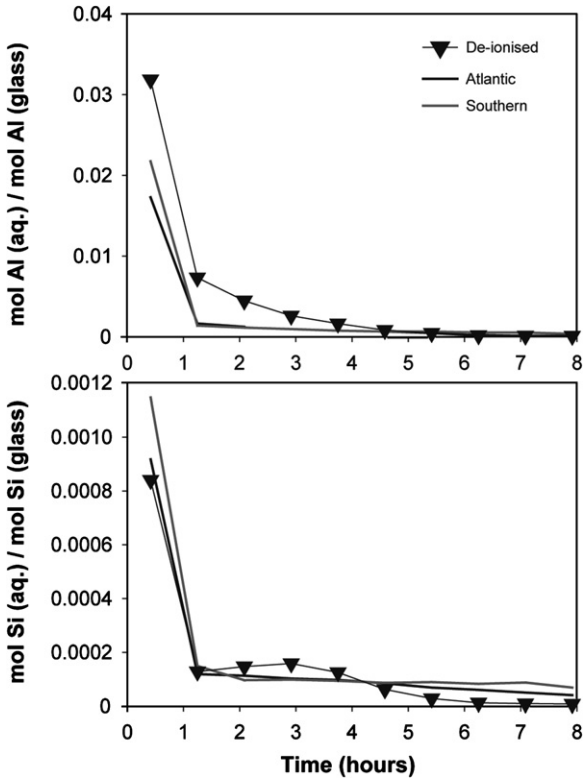

Fig. 10. The $Al_{(aqueous)}$:$Al_{(glass)}$ ratio (top) and $Si_{(aqueous)}$:$Si_{(glass)}$ ratio (bottom) through time when Hekla ash is mixed with deionized water and seawater.

Comparisons of element release in Fig. 10 and Table 3 imply that low pH conditions encourage elevated dissolution of some elements. In DI water, the differences between measured element fluxes and bulk dissolution rates strongly suggest that the dominant source of the dissolved elements is surface ash-leachates. In seawater, the contributions of bulk dissolution rates are heavily dependent of the timescale of the transient pH change. If surface waters have high concentrations of dissolved volatiles such as F, then it is possible to increase nutrient fluxes by elevating bulk dissolution rates. However, 5 g of ash only allowed an initial 40% increase in Si in 50 ml of seawater compared to DI water (Fig. 10), suggesting that the effects of mixing and diffusion in ocean surface waters will negate the impact of elevated bulk dissolution in seawater.

5. IMPLICATIONS

5.1. Fertilization potential

The high solubility of surface salts allows the immediate release of nutrients, which are initially concentrated in the

upper part of the water column. Previous studies have shown that this release occurs within minutes (Duggen et al., 2007). The fertilization potential of this nutrient flux is dependent on many factors. Eruption type and magnitude, deposition rates, ash particle size, and environmental buffering capacities will all influence nutrient flux rates from tephra. Ash-leachate dissolution can either instigate biological activity or lead to ecosystem stress if toxicity levels are breached (Smith and White, 1985; Frogner-Kockum et al., 2006). The utilization of volcanogenic nutrients depends on the biologically limiting factors of the ecosystem and whether the ash-leachate fluxes can be utilized by phytoplankton while the nutrients remain available in the surface waters. For example, timing of eruptions at high latitude is important where light can limit primary production and the oxidation of SO_2 (Gislason et al., 2002; Flaathen and Gislason, 2007).

Areas of oceans that are biologically limited by macronutrients (N and P) can be stimulated by ash deposition. Dissolved N as NO_2^-, NO_3^-, and NH_4^+ are released by a variety of ashes, as shown in this study and previous experiments (Duggen et al., 2007). Field observations have shown increases in marine primary productivity with concurrent increases in volcanically derived NH_3 (Uematsu et al., 2004). The Fe flux may affect N-limited surface waters because Fe is an important nutrient as a fixation pathway for N_2 and as a key element for several biogeochemical functions (Martin, 1990; Wu et al., 2000). If pulses of volcanogenic Fe are capable of increasing N_2 fixation, as seen in areas with elevated continuous Fe fluxes (Falkowski, 1997; Falkowski et al., 1998), then it is possible that substantial deposition of tephra could alter the bio-limiting nutrient(s) of an N-limited ecosystem.

Table 4 estimates the effect of three variables that can affect surface water enrichment; the variations in water composition, ash chemistry, and magnitude of ash deposition. Calculations assume ash-leachate volumes from values in Tables 2 and 3, that the ash reacts with the upper 10 m of surface waters, and that nutrient fluxes are largely unaffected by ash deposition rate and volume. Three magnitudes of ash deposition are considered, 0.1, 1, and 10 kg m^{-2}. These approximately correspond to ash layer thicknesses of 0.04, 0.4, and 4 mm, respectively.

The estimated P concentrations are relatively unaffected by deposition of subduction zone volcanic ash, as fluxes (positive and negative) are minor compared to background concentrations in ocean surface waters. Re-adsorption of P by Galeras and Montserrat ash when modeling a 4 mm ash blanket mixing with North Atlantic seawater generates a reduction in P concentrations of less than 2%. These estimations should be treated with some caution, given the dependence of P release on buffering capacities and saturation states of Fe oxides. In comparison, P release from Hekla is significant, increasing concentrations in all water types at high deposition volumes. This is likely to be due to the high F concentrations leaching tephra prior to deposition, and post-deposition in low pH conditions caused by the release of F.

Fe release from Galeras, Montserrat, and Santiaguito is relatively minor, with significant changes to background concentrations only occurring in high deposition volume scenarios. Hekla deposition at 0.1 kg m^{-2} (0.04 mm) increases background Fe concentrations by more than all but one of the subduction zone samples at deposition volumes of 10 kg m^{-2} (4 mm). Fe concentrations increase up to 9.1 μmol l^{-1} at 10 kg m^{-2} (4 mm), though such concentrations are unsustainable and will precipitate as Fe oxides within minutes in open ocean settings. This will limit the availability of Fe and reduce the fertilization potential.

Concentrations of micronutrients are affected more than macronutrients due to higher fluxes from ash samples relative to background concentrations. The predicted increases in micronutrient concentrations, even at low volumes of ash deposition, are substantially more than the Redfield-type element ratios of plankton organic tissue (Bruland et al., 1991):

16 N:1 P: 0.005 Fe: 0.002 Zn: 0.0004 Cu, Mn, Ni, Cd

Mn concentrations are particularly affected, increasing by two orders of magnitude in typical fresh water, coastal water and open ocean water for high deposition rates of Galeras, Montserrat, and Hekla ash (Table 4). The results suggest that surface waters that are micronutrient limited prior to ash deposition will see an increase in fertilization potential.

5.2. Potential of poisoning

Elements present in ash-leachates, including F, Al, Mn, Co, Ni, Cu, Zn, Cd, Ba, and Pb, can potentially inhibit biological growth (Brand et al.,1983, 1986; Sunda, 1988–1989; Bruland et al., 1991). Halogens, particularly F when found as F^- and HF, are particularly toxic to organisms with skeletal tissue (WHO, 1993; Witham et al., 2005). The toxicity of Al–F species in surface waters affected by the Hekla ash has been described by Frogner-Kockum et al. (2006) and Flaathen and Gislason (2007). To outline the poisoning potential of ash-leachates we focus on Cu, which is toxic to microorganisms when found as hydrated Cu^{2+} ions in surface waters and is released in significant quantities in this study and previous experiments (Duggen et al., 2007). The toxicity threshold for Cu^{2+} varies among phytoplankton phyla. Cyanobacteria appear most sensitive, while diatoms are most resistant (Brand et al., 1986). Concentrations of free Cu^{2+} above 10^{-11} mol l^{-1} can completely inhibit cyanobacteria growth rates (Brand et al., 1986; Buck and Bruland, 2005). Larvae of several zooplankton are affected at this concentration (Sunda et al., 1987; Sunda et al., 1990). The speciation of dissolved Cu varies with ecological system, with total hydrated Cu^{2+} bioavailability limited by the presence of strong binding organic ligands (Van den Berg et al., 1987; Donat et al., 1994; Moffett et al., 1997; Kozelka and Bruland, 1998; Buck and Bruland, 2005). Cyanobacteria and other organisms can produce Cu chelating ligands when under Cu stress (Moffett and Brand, 1996; Croot et al., 2000), suggesting that some of the volcanogenic Cu can be complexed by these organic ligands (Duggen et al., 2007).

The initial Cu fluxes from the ash samples vary from 1 to 49 nmol g^{-1} h^{-1} and are largely unaffected by varying

Table 4
Predicted changes to surface water nutrient levels due to ash deposition using mechanical mixing

		Initial conc. (nmol/kg)	Galeras			Montserrat			Hekla			Santiaguito		
			0.1 kg m^{-2} nmol/kg	1 kg m^{-2} nmol/kg	10 kg m^{-2} nmol/kg	0.1 kg m^{-2} nmol/kg	1 kg m^{-2} nmol/kg	10 kg m^{-2} nmol/kg	0.1 kg m^{-2} nmol/kg	1 kg m^{-2} nmol/kg	10 kg m^{-2} nmol/kg	0.1 kg m^{-2} nmol/kg	1 kg m^{-2} nmol/kg	10 kg m^{-2} nmol/kg
Icelandic river waterλ	P	**134**	134	136	152	134	136	149	156	352	2310	135	143	220
	Fe	**109**	110	121	226	109	113	150	218	1194	10963	109	110	123
	Zn	**8**	9	16	88	9	14	62	9	18	111	8	8	11
	Cu	**5.3**	5.6	8.4	36.7	5.7	9.5	47.8	5.4	6.4	16.7	5.3	5.4	6.8
	Mn	**6**	13	77	717	13	78	731	13	73	675	6	8	21
	Ni	**3.7**	3.9	6.3	29.7	3.8	4.6	12.8	3.7	4.5	12.2	3.7	4.1	8.4
	Cd	**0.03**	0.04	0.08	0.55	0.03	0.04	0.10	0.06	0.37	3.40	0.03	0.03	0.06
North Atlantic Ocean Water	P	**718**	718	717	703	718	717	711	722	755	1090	718	720	737
	Fe	**239**	239	244	286	240	249	341	310	948	7326	239	241	256
	Zn	**131**	132	137	188	131	134	159	132	139	208	131	131	129
	Cu	**6.0**	6.1	7.4	19.9	6.1	7.1	17.5	6.1	7.1	17.5	6.0	6.2	8.4
	Mn	**4**	10	62	584	9	58	544	11	76	723	11	76	723
	Ni	**8.0**	8.2	10.0	27.5	8.0	8.3	11.1	8.1	9.3	20.6	8.0	8.2	9.5
	Cd	**0.9**	0.9	0.9	1.4	0.9	0.9	1.0	0.9	1.2	4.3	0.9	09	0.9
Southern Ocean Water	P	**102**	102	102	103	102	105	130	106	138	461	102	104	118
	Fe	**0.3***	0.4	1	7	0.5	2	21	90	893	8923	0.7	5	42
	Zn	**0.03***	0.4	4.0	39.9	0.3	2.2	22.0	0.9	9.2	91.6	0.1	0.4	3.3
	Cu	**0.6***	0.7	1.9	13.5	0.7	1.3	7.1	0.7	1.5	9.8	0.6	0.9	3.9
	Mn	**4**	11	75	709	9	57	537	13	96	920	5	9	56
	Ni	**2.0**	2.2	4.1	23.5	2.0	2.3	4.9	2.0	2.2	4.4	2.0	2.2	3.9
	Cd	**0.02***	0.03	0.07	0.54	0.02	0.03	0.09	0.05	0.36	3.42	0.02	0.02	0.05

Estimates assume that ash deposition interacts with the top 10 m of surface waters, using the measured background concentrations in water samples. *Southern Ocean measurements taken in October 2000 by Michael Ellwood (NIWA). λBackground fresh water concentrations are the average composition (40 samples) of Fellsá, a river in eastern Iceland that drains an area with no hydrothermal input (Gislason et al., 2004). Element fluxes into river water are assumed to be measured the fluxes into de-ionized water.

solvent, suggesting a surface salt source. Mixing ratio estimates suggest that Cu concentrations can be trebled by large volumes of ash deposition (Table 4). Predicted speciation of volcanogenic Cu using PHREEQC suggests that initial concentrations of free Cu^{2+} can exceed 10^{-7} mol l^{-1} in fresh water, much higher than the toxicity threshold and damaging to organisms in the immediate vicinity (Brand et al., 1986). In ocean surface waters, toxicity thresholds depend on the ligands present prior to deposition, the amount of ligands released due to increases Cu stress, and the rate of diffusion and mixing through the water column. Heavy loading of volcanic ash in environments with low concentrations of organic ligands, such as open ocean surface waters and fresh water, could exceed the toxicity threshold of free Cu^{2+} and reduce biological activity (Brand et al., 1986; Duggen et al., 2007).

An important consideration for the toxicity potential of ash-leachates is changes to pH levels, increasing ecosystem stress. Sustained acidity increases the availability of toxic ions such as Cu^{2+} and Al^{3+}. Complexation of Al by organic acids is reduced in waters with low pH, allowing the bioavailable species AlF_x^{+3-x} to dominate. These dramatically increase the toxicity of Al to fish and other organisms. Concentrations over around 5×10^{-6} mol l^{-1} appear to be toxic to fish (Gensemer and Playle, 1999). PHREEQC predicts that free Al^{3+} in the reacted seawater samples reaches a maximum of 3.5 and 7×10^{-6} mol l^{-1} in the Galeras and Montserrat experiments, respectively, while mixing with Hekla ash only predicts initial speciation to reach 1.6×10^{-8} mol l^{-1} due to excess F allowing AlF_3 to dominate. Systems likely to be adversely affected by pH change are those with a low turnover rate and low buffering capacity. Terrestrial environments such as ponds, lakes, and soils would be affected by Al toxicity (Frogner-Kockum et al., 2006). The high buffering capacity of seawater will make the poisoning of ocean surface waters much more transient and less severe than in terrestrial environments, though mixing calculations suggest that moderate (5 kg m^{-2}, ~2 mm thick) ashfall from an eruption like Hekla could easily create transient pH < 6 conditions in upper ocean surface waters.

Decreases in marine pH have been shown to have a large impact on organisms dependent on calcium carbonate for shell or skeleton formation (Feely et al., 2004; Orr et al., 2005; Ridgwell et al., 2007; Riebesell et al., 2000; Royal Society, 2005). The majority of biogenic carbonate precipitation is carried out by microorganisms (Milliman, 1993), suggesting that a decline of calcifying organisms could have large implications for the carbon cycle, as well as food web structure and health. Significant decreases to ocean pH lowers carbonate ion concentrations, thereby altering $CaCO_3$ saturation (Orr et al., 2005). The $CaCO_3$ polymorphs aragonite and calcite are the dominant forms used for shell building. Both polymorphs are currently stable in today's surface waters as conditions are supersaturated. However, decreasing pH reduces availability of CO_3^{2-}, leading to possible undersaturation. Aragonite is the least stable, reaching saturation at pH 7.8 (Orr et al., 2005). In undersaturated conditions, calcifying organisms show reduced calcification rates, malformation, and enhanced dissolution of shells in both temperate and tropical waters (Gattuso et al., 1998; Langdon et al., 2000; Riebesell et al., 2000).

The large pH decreases observed in seawater experiments (Fig. 5) suggest that surface water conditions post-eruption could approach undersaturation for both aragonite and calcite, depending on the extent of diffusion and mixing. Analysis of saturation states, using the PHREEQC program, predicts that aragonite and calcite become undersaturated for Hekla, Montserrat, and Galeras ash samples at the 60 ml l^{-1} flow rate. Total free CO_3^{2-} is closely linked to pH and is initially reduced to nanomolar concentrations after initial contact with Hekla ash, causing undersaturation of both $CaCO_3$ polymorphs. This effect will be temporary as diffusion and mixing will initiate the change of HCO_3^- to CO_3^{2-} to compensate for CO_3^{2-} removal. While the ratio of ash to water in these experiments exaggerates the scale of change, rapid deposition of volatile bearing tephra could cause temporary undersaturation of $CaCO_3$. This would increase ecosystem stress for calcifying organisms. Deposition of ash-leachates into colder waters increases the likelihood of undersaturation as average CO_3^{2-} concentrations are generally lower due to temperature and upwelling differences (Orr et al., 2005).

Evidence of poisoning in oceanic surface waters has recently been observed within marine sediment cores from the Caribbean Sea around Montserrat (Palmer, 2007). Within the cores collected a layer, up to 5 mm thick and comprised solely of pteropod shells, was found by M.B. Hart and J.K. Fisher at the base of a recent ashfall deposit. This ash fall, located to the west–northwest of the island, and sampled in cores situated 10–20 km from the coast of Montserrat, formed from recent fall out of ash from the volcano. The close inter-correlation between the pteropod layer and the overlying ash deposit suggest the fate of these gastropods was related to the ash deposition. Similar pteropod layers were not found associated with the more common submarine flow deposits around the island (Trofimovs et al., 2007), though this may be due to the destruction of shells during emplacement. It is not clear how the pteropods died en masse, though it is possible that ash-leachate release in upper surface waters lead to toxic and/or acidic conditions that immediately killed the pteropods. Alternatively, when disturbed many pteropods withdraw into their shells and sink through the water column. Continued ash fall would result in them sinking into deeper water than they normally occupy in life, with fatal results (Lalli and Gilmer, 1989). Pteropod shells are made of aragonite, so transient acidification would have etched the shells. However, using this as a test for proof of surface water acidification may be complicated by subsequent etching caused as the tests settle through the water column and by subsequent diagenesis on the sea floor, beneath the ash layer.

Uncertainties associated with the biological response to ash-leachate release and the interaction with the N and C cycles mean that predictions of an enhanced carbon rain ratio through volcanic nutrient addition are speculative. Diminished CO_3^{2-} availability hampers calcification rates, which is the main ballast for organic carbon (Klaas and Archer, 2002). A reduction of CO_3^{2-} would hinder, or possibly even inhibit, sedimentation of deceased organisms

out of surface waters. Alternative ballast in the form of ash particles could allow CO_2 transport to depth, but these processes have not been investigated. Further work needs to consider these processes when assessing the impact of volcanic ash deposition on oceanic and atmospheric CO_2 levels.

6. CONCLUSIONS

Volcanic ash from a variety of volcanoes release high concentrations of volatiles, nutrients, and metals in both de-ionized and ocean surface waters. Certain element fluxes, especially P and Al, are elevated in DI water. However, most elements show comparable release with varying solvent. Unhydrated tephra with high F concentrations, such as Hekla ash, cause 1–2 order of magnitude increases in fluxes of important nutrients including Si, P, and Fe. The likely source for these elevated fluxes is leaching of host particles by F, though this process occurs before contact with water. In the absence of high F concentrations and for most other nutrients, the governing contributor to element release is adsorbed surface metal salts and aerosols.

Deposition and subsequent dissolution of ash-leachates in surface waters have the potential to cause biogeochemical changes. Findings from this study compliment previous deductions concerning the fertilization potential of volcanic ash in surface waters (Duggen et al., 2007; Frogner et al., 2001). We evaluate the variation in ash-leachate toxicity with water chemistry, showing that transient drops in pH can occur in all solvents given sufficient magnitudes of ash deposition. Surface water acidification and/or the release of toxic elements may hinder any increases in primary productivity and the rain of organic carbon to depth, offsetting the predicted impact of volcanogenic fertilization on atmospheric CO_2 levels. The relative impacts on biodiversity from ash-leachate release depend on the season of eruption, latitude, eruption volume and intensity, ash-leachate speciation, and surface water chemistry. If certain organisms are prone to rapid fluxes of metal salts from tephra, such as the pteropods found west of Montserrat, then a shift within the ecosystem to more robust organisms is expected. In the absence of a toxicity threshold being breached, ash-leachate deposition should instigate an increase in primary productivity, limited by the least available macronutrient. These processes are still too poorly understood to make definite predictions about the fate of calcifying organisms and the potential sequestration of atmospheric CO_2.

ACKNOWLEDGMENTS

Gloria Cortés, Michael Ellwood, Paul Frogner, Claire Horwell, Sue Loughlin, Bill Rose, and Derek Vance are thanked for helping with sample collection. Simon Cobb, Therese Flaathen, Ingvi Gunnarsson, Bergur Sigfússon, the Icelandic Marine Research Institute, and the British Geological Survey Analytical Geochemistry Laboratories assisted with sample analyses. Many thanks are due to Svend Duggen, Daniela Schmidt, Steve Sparks, Derek Vance and an anonymous reviewer for constructive criticisms and comments that have improved this work, and to Jeffrey Alt for handling this manuscript. Morgan Jones was supported by a NERC studentship.

APPENDIX A. SUPPLEMENTARY DATA

Supplementary data associated with this article can be found, in the online version, at doi:10.1016/j.gca.2008.05.030.

REFERENCES

Africano F., Van Rompaey G., Bernard A. and Le Guern F. (2002) Deposition of trace elements from high temperature gases of Satsuma-Iwojima volcano. *Earth Planets Space* **54**, 275–286.

Armienta M. A., Cruz-Renya S. D. l., Morton O., Cruz O. and Ceniceros N. (2002) Chemical variations of tephra-fall deposit leachates for three eruptions from Popocatepetl volcano. *J. Volcanol. Geothermal Res.* **113**, 61–80.

Bernard A. and Le Guern F. (1986) Condensation of volatile elements in high-temperature gases of Mount St. Helens. *J. Volcanol. Geothermal Res.* **28**, 91–105.

Bluth G. and Rose W. (2004) Observations of eruptive activity at Santiaguito Volcano, Guatemala. *J. Volcanol. Geothermal Res.* **136**, 297–302.

Boyd P., Watson A., Law C., Abraham E., Trull T., Murdoch R., Bakker D., Bowie A., Buesseler K., Chang H., Charette M., Croot P., Downing K., Frew R., Gall M., Hadfield M., Hall J., Harvey M., Jameson G., LaRoche J., Liddicoat M., Ling R., Maldonado M., McKay R., Nodder S., Pickmere S., Pridmore R., Rintoul S., Safi K., Sutton P., Strzepek R., Tanneberger K., Turner S., Waite A. and Zeldis J. (2000) A mesoscale phytoplankton bloom in the polar Southern Ocean stimulated by iron fertilization. *Nature* **407**, 695–702.

Brand L. E., Sunda W. G. and Guillard R. R. L. (1983) Limitation of marine phytoplankton reproductive rates by zinc, manganese, and iron. *Limnol. Oceanogr.* **28**, 1182–1195.

Brand L. E., Sunda W. G. and Guillard R. R. L. (1986) Reduction of marine phytoplankton reproductive rates by copper and cadmium. *J. Exp. Mar. Biol. Ecol.* **96**, 225–250.

Brantley S., White A. and Hodson M. (1999) Surface area of primary silicate minerals. In *Growth, Dissolution and Pattern Formation in Geo-systems* (eds. B. Jamtveit and P. Meakin). Chapman & Hall, London.

Bruland K. W., Donat J. R. and Hutchins D. A. (1991) Interactive influences of bioactive trace metals on biological production in oceanic waters. *Limnol. Oceanogr.* **36**, 1555–1577.

Buck K. and Bruland K. (2005) Copper speciation in San Francisco Bay: a novel approach using multiple analytical windows. *Mar. Chem.* **96**, 185–198.

Calvache M. and Williams S. (1997) Geochemistry and petrology of the Galeras Volcanic Complex, Colombia. *J. Volcanol. Geothermal Res.* **77**, 21–38.

Carey S. (1997) Influence of convective sedimentation on the formation of widespread tephra fall layers in the deep sea. *Geology* **25**, 839–842.

Croot P. L., Moffett J. W. and Brand L. (2000) Production of extracellular Cu complexing ligands by eucaryotic phytoplankton in response to Cu stress. *Limnol. Oceanogr.* **45**, 619–627.

Delmelle P., Gerin P. and Oskarsson N. (2000) Surface and bulk studies of leached and unleached volcanic ashes. *EOS, Trans. Am. Geophys. Union* **81**, F1311.

Delmelle P., Lambert M., Dufrene Y., Gerin P. and Oskarsson N. (2007) Gas/aerosol-ash interaction in volcanic plumes: new insights from surface analyses of fine ash particles. *Earth Planet. Sci. Lett.* **259**, 159–170.

Donat J., Lao K. and Bruland K. (1994) Speciation of dissolved copper and nickel in South San Francisco Bay: a multi-method approach. *Anal. Chim. Acta* **284**, 547–571.

Duggen S., Croot P., Schacht U. and Hoffmann L. (2007) Subduction zone volcanic ash can fertilize the surface ocean and stimulate phytoplankton growth: evidence from biogeochemical experiments and satellite data. *Geophys. Res. Lett.* **34**, L01612.

Falkowski P., Barber R. and Smetacek V. (1998) Biogeochemical controls and feedbacks on ocean primary production. *Science* **281**, 200–206.

Falkowski P. G. (1997) Evolution of the nitrogen cycle and its influence on the biological sequestration of CO_2 in the ocean. *Nature* **387**, 287.

Feely R., Sabine C., Lee K., Berelson W., Kleypas J., Fabry V. and Millero F. (2004) Impact of anthropogenic CO_2 on the $CaCO_3$ system in the Oceans. *Science* **305**, 362–366.

Flaathen T. K. and Gislason S. R. (2007) The effect of volcanic eruptions on the chemistry of surface waters: the 1991 and 2000 eruptions of Mt. Hekla, Iceland. *J. Volcanol. Geothermal Res.* **164**, 293–316.

Frogner-Kockum P. C., Herbert R. B. and Gislason S. R. (2006) A diverse ecosystem response to volcanic aerosols. *Chem. Geol.* **231**, 57–66.

Frogner P., Gislason S. R. and Oskarsson N. (2001) Fertilizing potential of volcanic ash in ocean surface water. *Geology* **29**, 487–490.

Gattuso J.-P., Frankignoulle M., Bourge I., Romaine S. and Buddemeier R. (1998) Effect of calcium carbonate saturation of seawater on coral calcification. *Global Planet. Change* **18**, 37–46.

Gautier J.-M., Oelkers E. and Schott J. (2001) Are quartz dissolution rates proportional to BET surface areas? *Geochim. Cosmochim. Acta* **65**, 1059–1070.

Gensemer R. W. and Playle R. C. (1999) The bioavailability and toxicity of aluminum in aquatic environments. *Environ. Sci. Technol.* **29**, 315–450.

Gislason S. and Eugster H. (1987) Meteoric water-basalt interactions: I. A laboratory study. *Geochim. Cosmochim. Acta* **51**, 2827–2840.

Gislason S., Snorrason Á., Kristmannsdóttir H., Sveinbjörnsdóttir Á., Torsander P., Ólafsson J., Castet S. and Dupré B. (2002) Effects of volcanic eruptions on the CO_2 content of the atmosphere and the oceans: the 1996 eruption and flood within the Vatnajökull Glacier, Iceland. *Chem. Geol.* **190**, 181–205.

Gislason S. R. and Oelkers E. H. (2003) Mechanism, rates and consequences of basaltic glass dissolution: II. An experimental study of the dissolution rates of basaltic glass as a function of pH and temperature. *Geochim. Cosmochim. Acta* **67**, 3817–3832.

Gislason S. R., Snorrason Á., Eiríksdóttir E. S., Sigfússon B., Elefson S. Ó., Harðardóttir J., Gunnarsson Á., Hreinsson E. Ö., Torssander P., Óskarsson N. Ö. and Oelkers E. H. (2004). *Efnasamsetning, rennsli og aurburður straumvatna á Austurlandi.*

Graedel T. E. and Franey J. P. (1975) Field measurements of submicron aerosol washout by snow. *Geophys. Res. Lett.* **2**, 325–328.

Horwell C., Fenoglio I. and Fubini B. (2007) Iron-induced radical generation from basaltic volcanic ash. Earth Planet. Sci. Lett. doi:10.1016/j.epsl.2007.07.032.

Kelly P., Jones P. and Jia P. (1996) The spatial response of the climate system to explosive volcanic eruptions. *Intl. J. Climatol.* **16**, 537–550.

Klaas C. and Archer D. (2002) Association of sinking organic matter with various types of mineral ballast in the deep sea: implications for the rain ratio. *Global Biogeochem. Cycles* **16**. doi:10.1029/2001GB001765.

Kozelka P. and Bruland K. (1998) Chemical speciation of dissolved Cu, Zn, Cd, Pb in Narragansett Bay, Rhode Island. *Mar. Chem.* **60**, 267–282.

Lalli C. M. and Gilmer R. W. (1989) Pelagic Snails: The Biology of Holoplanktonic Gastropod Molluscs. Stanford University Press, California.

Langdon C., Takahashi T., Sweeney C., Chipman D., Goddard J., Marubini F., Aceves H., Barnett H. and Atkinson M. (2000) Effect of calcium carbonate saturation state on the calcification rate of an experimental coral reef. *Global Biogeochem. Cycles* **14**, 639–654.

Le Bas M., Le Maitre R. and Woolley A. (1991) The construction of the total alkali-silica chemical classification of volcanic rocks. *Mineral. Petrol.* **46**, 1–22.

Martin J. (1990) Glacial-interglacial CO_2 change: the iron hypothesis. *Paleoceanography* **5**, 1–13.

Martin J. H., Coale K. H., Johnson K. S., Fitzwater S. E., Gordon R. M., Tanner S. J., Hunter C. N., Elrod V. A., Nowicki J. L., Coley T. L., Barber R. T., Lindley S., Watson A. J., Scoy K. v., Law C. S., Liddicoat M. I., Ling R., Stanton T., Stockel J., Collins C., Anderson A., Bidigare R., Ondrusek M., Latasa M., Millero F. J., Lee K., Yao W., Zhang J. Z., Friedrich G., Sakamoto C., Chavez F., Buck K., Kolber Z., Greene R., Falkowski P., Chisholm S. W., Hoge F., Swift R., Yungel J., Turner S., Nightingale P., Hatton A., Liss P. and Tindale N. W. (1994) Testing the iron hypothesis in ecosystems of the equatorial Pacific Ocean. *Nature* **371**, 123–129.

Milliman J. (1993) Production and accumulation of calcium carbonate in the ocean: budget of a nonsteady state. *Global Biogeochem. Cycles* **7**, 927–957.

Moffett J., Brand L., Croot P. and Barbeau K. (1997) Cu speciation and cyanobacterial distribution in harbors subject to anthropogenic Cu inputs. *Limnol. Oceanogr.* **42**, 789–799.

Moffett J. W. and Brand L. E. (1996) Production of strong, extracellular Cu chelators by marine cyanobacteria in response to Cu stress. *Limnol. Oceanogr.* **41**, 388–395.

Moune S., Gauthier P.-J., Gislason S. R. and Sigmarsson O. (2006) Trace element degassing and enrichment in the eruptive plume of the 2000 eruption of Hekla volcano, Iceland. *Geochim. Cosmochim. Acta* **70**, 461–479.

Oelkers E. and Gislason S. (2001) The mechanism, rates and consequences of basaltic glass dissolution: I. An experimental study of the dissolution rates of basaltic glass as a function of aqueous Al, Si and oxalic acid concentration at 25 °C and pH = 3 and 11. *Geochim. Cosmochim. Acta* **65**, 3671–3681.

Oppenheimer C. (2003) Volcanic degassing. In *The Crust* (ed. R. L. Rudnick). Elsevier-Pergamon, Oxford.

Orr J., Fabry V., Aumont O., Bopp L., Doney S., Feely R., Gnanadesikan A., Gruber N., Ishida A., Joos F., Key R., Lindsay K., Maier-Reimer E., Matear R., Monfray P., Mouchet A., Najjar R., Plattner G.-K., Rodgers K., Sabine C., Sarmiento J., Schlitzer R., Slater R., Totterdell I., Weirig M.-F., Yamanaka Y. and Yool A. (2005) Anthropogenic ocean acidification over the twenty-first century and its impact on calcifying organisms. *Nature* **437**, 681–686.

Oskarsson N. (1980) The interaction between volcanic gases and tephra: fluorine adhering to tephra of the 1970 Hekla eruption. *J. Volcanol. Geothermal Res.* **8**, 251–266.

Palmer M. R. (2007) Impact of the Early Diagenesis of Sub-aerial Volcanic Material in the Marine Environment RRS James Cook Cruise 18 Report. University of Southampton.

Parkhurst D. and Appelo C. (1999) User's guide to PHREEQC (version 2)—a computer program for speciation, batch-reaction, one-dimensional transport, and inverse geochemical

calculations. *Water-Resource Investigation Report 99-4259*. US Geological Survey.

Ridgwell A., Zondervan I., Hargreaves J., Bijma J. and Lenton T. (2007) Assessing the potential long-term increase of oceanic fossil fuel CO_2 uptake due to CO_2-calcification feedback. *Biogeosciences* **4**, 481–492.

Riebesell U., Zondervan I., Rost B., Tortell P., Zeebe R. and Morel F. (2000) Reduced calcification of marine phytoplankton in response to increased atmospheric CO_2. *Nature* **407**, 364–367.

Riese A. C. (1982) Adsorption of radium and thorium onto quartz and kaolinite: a comparison of solution/surface equilibria models. PhD Thesis, Colarado School of Mines.

Risacher F. and Alonso H. (2001) Geochemistry of ash leachates from the 1993 Lascar eruption, northern Chile. Implication for recycling of ancient evaporites. *J. Volcanol. Geothermal Res.*, 109.

Robock A. (2000) Volcanic eruptions and climate. *Rev. Geophys.* **38**, 191–219.

Rose W. I. (1977) Scavenging of volcanic aerosol by ash: atmospheric and volcanologic implications. *Geology* **5**, 621–624.

Royal Society. (2005) Ocean acidification due to increased atmospheric carbon dioxide. The Royal Society, London.

Sarmiento J. L. (1993) Atmospheric CO_2 stalled. *Nature* **365**, 697–698.

Smith D. B., Zielinski G. A. and Rose W. I. (1982) Leachability of uranium and other elements from freshly erupted volcanic ash. *J. Volcanol. Geothermal Res.* **13**, 1–30.

Smith M. A. and White M. J. (1985) Observations on Lakes near Mount St. Helens: phytoplankton. *Arch. Fuer Hydrobiol.* **104**, 345–362.

Stefánsdóttir M. and Gislason S. (2005) The erosion and suspended matter/seawater interaction during and after the 1996 outburst flood from the Vatnajökull Glacier, Iceland. *Earth Planet. Sci. Lett.* **237**, 433–452.

Sunda W. (1988–1989) Trace metal interactions with marine phytoplankton. *Biol. Oceanogr.* **6**, 411–442.

Sunda W., Tester P. and Huntsman S. (1987) Effects of cupric and zinc ion activities on the survival and reproduction of marine copepods. *Mar. Biol.* **94**, 203–210.

Sunda W., Tester P. and Huntsman S. (1990) Toxicity of trace metals to *Acartia tonsa* in the Elizabeth River and Southern Chesapeake Bay. *Estuarine Coastal Shelf Sci.* **30**, 207–221.

Tester J., Worley W., Robinson B., Grigsby C. and Feerer J. (1994) Correlating dissolution kinetics in pure water from 25 to 625 °C. *Geochim. Cosmochim. Acta* **58**, 2407–2420.

Trofimovs J., Sparks R. S. J. and Talling P. J. (2007) Anatomy of a submarine pyroclastic flow and associated turbidity current: July 2003 dome collapse, Soufriere Hills volcano, Montserrat, West Indies. *Sedimentology*. doi:10.1111/j.1365-3091.2007.00914.x.

Uematsu M., Toratani M., Kajino M., Narita Y., Senga Y. and Kimoto T. (2004) Enhancement of primary productivity in the western North Pacific caused by the eruption of the Miyake-jima Volcano. *Geophys. Res. Lett.* **31**, 1–4.

Van den Berg C., Merks A. and Duursma E. (1987) Organic complexation and its control of the dissolved concentrations of copper and zinc in the Scheldt Estuary. *Estuarine Coastal Shelf Sci.* **24**, 785–797.

Varekamp J. C., Luhr J. F. and Prestegaard K. L. (1984) The 1982 eruptions of El Chichón Volcano (Chiapas, Mexico): character of the eruptions, ash-fall deposits, and gas phase. *J. Volcanol. Geothermal Res.* **23**, 39–68.

Watson A. (1997) Volcanic Fe, CO_2, ocean productivity and climate. *Nature* **385**, 587–588.

WHO. (1993) *Guidelines for Drinking-water Quality*. World Health Organization, Geneva.

Wiesner M., Wang Y. and Lianfu Z. (1995) Fallout of volcanic ash to the deep South China Sea induced by the 1991 eruption of Mount Pinatubo (Philippines). *Geology* **23**, 885–888.

Williams J. D. H., Jacquet J. M. and Thomas R. L. (1976) Forms of phosphorus in surficial sediments of Lake Erie. *J. Fisheries Res. Board Canada* **33**, 413–429.

Witham C., Oppenheimer C. and Horwell C. (2005) Volcanic ash-leachates: a review and recommendations for sampling methods. *J. Volcanol. Geothermal Res.* **141**, 299–326.

Wolff-Boenisch D. (2004). *Data on 17 Icelandic volcanic glasses and 1 Californian ignimbrite*. .

Wolff-Boenisch D., Gislason S. R. and Oelkers E. (2004a) The effect of fluoride on the dissolution rates of natural glasses at pH 4 and 25 °C. *Geochim. Cosmochim. Acta* **68**, 4571–4582.

Wolff-Boenisch D., Gislason S. R., Oelkers E. and Putnis C. (2004b) The dissolution rates of natural glasses as a function of their composition at pH 4 and 10.6, and temperatures from 25 to 74 °C. *Geochim. Cosmochim. Acta* **68**, 4843–4858.

Wu J., Sunda W. G., Boyle E. A. and Karl D. M. (2000) Phosphate depletion in the Western North Atlantic Ocean. *Science* **289**, 759–762.

Associate editor: Jeffrey C. Alt